cosmetics

MDPI

Article

Preparation and Characterization of Callus Extract from *Pyrus pyrifolia* and Investigation of Its Effects on Skin Regeneration

Dae Eung Park †, Deepak Adhikari †, Rudra Pangeni, Vijay Kumar Panthi, Hyun Jung Kim * and Jin Woo Park *

College of Pharmacy and Natural Medicine Research Institute, Mokpo National University, Muan-gun, Jeonnam 58554, Korea; da3125@naver.com (D.E.P.); dpak7adh@gmail.com (D.A.); capriconpangeni@gmail.com (R.P.); nepalivijay7@gmail.com (V.K.P.)

* Correspondence: hyunkim@mokpo.ac.kr (H.J.K.); jwpark@mokpo.ac.kr (J.W.P.); Tel.: +82-61-450-2686 (H.J.K.); +82-61-450-2704 (J.W.P.)

† These authors contributed equally to this work.

Received: 1 November 2018; Accepted: 12 December 2018; Published: 15 December 2018

Abstract: In the present study, an aqueous extract was prepared using calli from the in vitro-derived leaves of *Pyrus pyrifolia* cultured in Murashige and Skoog medium containing picloram for a plant growth regulator. The major biological components in the callus extract were identified as uridine (**1**), adenosine (**2**), and guanosine (**3**). In terms of the antioxidant activity, at 300 μg/mL, the extract exhibited free radical scavenging activity of 76.9% ± 2.88% in the 2,2-diphenyl-1-picrylhydrazyl (DPPH) assay, comparable to that of 44 μg/mL ascorbic acid (82.5% ± 3.63%). In addition, the IC_{50} values for inhibition of advanced glycation end product formation from collagen and elastin were 602 ± 2.72 and 3037 ± 102.5 μg/mL, respectively. The extract significantly promoted keratinocyte and fibroblast cell proliferation in a dose-dependent manner. Moreover, fibroblasts treated with 1.36 μg/mL extract exhibited a 1.60-fold increase in procollagen type I C-peptide level compared to controls. The in vitro wound recovery rates of keratinocytes and fibroblasts were also 75% and 38% greater, respectively, than those of serum-free controls at 9 and 36 h after extract treatment (1.36 μg/mL). Additionally, the extract flux across the human epidermis increased by 1598% after its incorporation into elastic nanoliposomes (NLs). Therefore, elastic NLs loaded with *Pyrus pyrifolia* callus extract have potential use as skin rejuvenators and antiaging ingredients in cosmetic formulations.

Keywords: *Pyrus pyrifolia*; callus extract; skin regeneration; topical delivery; antiaging cosmetics

1. Introduction

Cutaneous aging is a complicated biological process caused by various intrinsic and extrinsic factors, which bring about gradual destruction of structural integrity of the skin as well as its physiological functions [1,2]. Extrinsic aging involves a number of factors, such as continuous exposure to environmental insults, e.g., ultraviolet (UV) radiation. Such insults result in oxidative damage to the lipids, proteins, and DNA of the skin via the generation of free radicals that provoke cross-liking of collagen, thus leading to a loss of skin elasticity. Free radicals also damage the dermal connective tissue, resulting in premature skin aging (photoaging) [3–5]. Furthermore, persistent exposure to reactive oxygen species (ROS) has been shown to initiate skin aging, including wrinkle formation and melanogenesis [6]. The origin of intrinsic aging is commonly called the "biological clock." One theory is based on the observation that diploid cells, such as fibroblasts, have a finite lifespan in culture [7,8].

This results in cellular senescence, leading to altered gene expression and then to degenerative changes in tissues. Another intrinsic mechanism that contributes to skin aging is damage due to free radicals accumulated during the lifespan of an individual [9].

The Maillard glycation theory is a further general mechanism of intrinsic aging. Accumulation of the reaction products of protein glycation, produced by nonenzymatic reaction of proteins with glucose or other reducing sugars in living organisms, can induce structural and functional modifications of tissue proteins [10]. Many studies have demonstrated a significant role of glycation in the normal aging process as well as in the pathogenesis of aging-related diseases, such as diabetes, atherosclerosis, end-stage renal disease, rheumatoid arthritis, and neurodegenerative diseases [11–13]. Moreover, glycation has several adverse effects on the characteristics of collagen. The accumulation of Maillard reaction products has been shown to lead to stiffer and more brittle collagen, with consequent influences on the properties of the extracellular matrix (ECM) and ECM–cell interactions [14,15]. Thus, targeting glycation should have broad and beneficial effects on aging and aging-related diseases.

The pear, *Pyrus pyrifolia*, is one of the most widely consumed fruits in the world and has also been used as folk medicine in Korea and China because of its biological activities, including antitussive, anticonstipative, antiulcer, and antioxidative effects [16–20]. In addition, many phenolic compounds, such as arbutin, chlorogenic acid, quercetin, catechins, kaempferol, and procyanidins, have been characterized in pear fruits, and various hydroxycinnamoyl malic acids and their ethyl esters, hydroxycinnamoyl malates, procyanidins, and triterpenes have also been found in pear peel [21–26]. In particular, steroids (β-sitosterol, daucosterol, and α-amyrin), quercitrin, and triterpenoids (oleanolic acid, ursolic acid, and 2β,19α-hydroxyurosolic acid) have been isolated and identified as anti-inflammatory and/or antimicrobial compounds in *Pyrus bretschneideri* R. (Chinese pear) [16,17]. The aqueous ethanoic extract of the bark from *P. pyrifolia* was also shown to have positive glycation inhibitory and antioxidative efficacies [27].

Plant resources have long been studied as natural antioxidants and enzyme inhibitors related to inflammation, melanin hyperpigmentation, and a variety of skin disorders. Therefore, these resources are valuable in cosmetic formulations which aim to inhibit or impede oxidative damage to collagen induced by free radicals [28]. Antioxidants, including various bioactive compounds derived from natural products, have been applied to inhibit aging. However, the provision of fresh materials, regardless of the season and the plant reproductive cycle, have always been barriers to their application in the pharmaceutical and cosmetics industries. These factors make the extraction of bioactive compounds from plant sources highly inefficient and emphasize the need for novel approaches to produce their secondary metabolites. To overcome these limitations, in vitro plant tissue and cell culture have been suggested as valid alternatives [28–31]. The in vitro propagation and cell suspension cultures not only offer viable methods for the mass multiplication of scarce and endangered species, but are also important in the quality-controlled production of desired plant-derived bioactive components, including secondary metabolites with high levels of uniformity from batch to batch without risk of pathogenic or environmental contamination and for screening of natural inhibitors against various biological disorders [32,33]. Thus, plant cell culture represents an efficient way to produce several valuable natural products, such as commercially important products, including pigments (e.g., anthocyanins and betacyanins) and anti-inflammatory agents (e.g., berberine and rosmarinic acid) [33,34].

Extracts from plant cell cultures also include a board range of active ingredients, and in many cases they are present in high concentrations compared with those produced in vivo. However, for use in topically applied cosmetic products, bioactive compounds for preventing skin aging should be well tolerated and nonirritating, with no toxicity or side effects. In addition, the active compounds should be able to penetrate into the desired site of action across the stratum corneum (SC), and ultimately reach the living parts of the epidermis and/or dermis where glycation exhibits its harmful effects. Therefore, many studies have attempted to enhance the efficacy, stability, and solubility of bioactive compounds present in the plant extracts by incorporating them into colloidal systems, such as nanostructured lipid

carriers including solid lipid nanoparticles, polymeric nano-sized micelles, and microemulsions and nanoemulsions, to facilitate their skin penetration and/or protect them from degradation [35].

To produce various bioactive compounds, this study aimed to prepare and characterize an aqueous extract of *P. pyrifolia* callus as an antiaging cosmetic ingredient. In addition, topical nanocarriers based on nanoliposomes (NLs) were designed to enhance skin permeation of the callus extract. Calli were established from leaf explants of *P. pyrifolia* under controlled conditions, and molecular markers in the aqueous extract from in vitro-derived calli were identified by liquid chromatography mass spectrometry (LC-MS). Thereafter, the antioxidant activity of the callus extract was characterized by 1,1-diphenyl-2-picrylhydrazyl (DPPH) and 2,2′-azinobis-(3-ethylbenzoline-6-sulfonate) (ABTS) free radical scavenging assays, and the reduction of transition metal ions by ferric-reducing antioxidant power (FRAP) test. In addition, the inhibitory effect of the callus extract on ECM protein glycation was assessed by collagen and elastin glycation assays. To evaluate the skin regeneration efficacy of the *P. pyrifolia* callus extract, its abilities to stimulate proliferation and migration of keratinocytes and fibroblasts, followed by promotion of collagen synthesis by human fibroblasts, were measured. Finally, improvement of the skin permeability of the callus extract was assessed after its incorporation into elastic NLs.

2. Materials and Methods

2.1. Materials

Murashige and Skoog (M&S) medium, picloram, 2,4-dichlorophenoxyacetic acid, and 6-benzylaminopurine were purchased from Duchefa Bohemia B.V. (Haarlem, The Netherlands). Uridine, adenosine, and guanosine were obtained from Tokyo Chemical Industry Co. Ltd. (Tokyo, Japan). DPPH, ABTS, potassium persulfate, 2,4,6-tris(2-pyridyl)-s-triazine (TPTZ), ascorbic acid, $FeCl_3$, $FeSO_4$, cholesterol, and polysorbate 80 (Tween 80) were purchased from Sigma-Aldrich (St. Louis, MO, USA). Hydrogenated lecithin (Lipoid P75-3) and hydrogenated phosphatidylcholine (Lipoid P100-3) were provided by Lipoid (Ludwigshafen, Germany). Other chemicals were obtained from Merck KGaA (Darmstadt, Germany) and Thermo Fisher Scientific (Waltham, MA, USA).

2.2. Preparation and Characterization of P. pyrifolia Callus Extract

2.2.1. Preparation of Plant Material

P. pyrifolia plant seeds were soaked in pure water overnight and then immersed in 70% (*v/v*) ethanol for 90 s. After sterilizing their surfaces with a 4% (*w/v*) sodium hypochlorite solution for 15 min, the seeds were grown aseptically in M&S basal medium supplemented with 3% (*w/v*) sucrose and 0.4% (*w/v*) gelite. The pH of the medium was adjusted to 5.8 with 1 N NaOH before autoclaving at 121 °C for 15 min. Next, the seeds were maintained up to sprouting for 16 h in the light (2000 lx; 25 °C ± 1 °C) and 8 h in the dark (16 °C ± 1 °C) for 3–7 days. To induce callus formation, a 5 × 5-mm wound was created on the young leaves from the germination using a scalpel and placed onto M&S medium containing 3% (*w/v*) sucrose and 0.26% (*w/v*) gelite in combination with growth regulator (2 mg/L of picloram), followed by incubation in the dark at 26 °C ± 2 °C for 8 weeks. After collecting the calli, they were transplanted in the fresh M&S medium with 2 mg/L of picloram, and further incubated in the dark in a growth chamber at 26 °C ± 2 °C for 4 weeks. To raise the biomass of callus, cell suspension cultures were initiated by cultivating the calli in 500-mL flasks with 200 mL of M&S medium containing 3% (*w/v*) sucrose and 2 mg/L of picloram on a rotary shaker (120 rpm) in the dark at 25 °C ± 1 °C and then subcultured once every 3 weeks. After gathering and air-drying the calli at 50 °C, they were pulverized into a fine powder. Next, an aqueous callus extract was prepared by boiling 200 g of the callus powder in 1 L of water for 4 h, followed by filtration through a filter paper (pore size: 0.4 μm) and freeze-drying.

2.2.2. Isolation and Identification Procedure

The dried extract (9.98 g) was separated by flash chromatography using RP cartridges (120 g, KP-C18-HS; Biotage, Uppsala, Sweden) and eluted with methanol-water mixture (0:100 to 40:60) for 60 min at 40 mL/min to afford 13 fractions. Fractions 3–6 were further purified with a semi-preparative high-performance liquid chromatography (HPLC) system composed of a Waters 600 HPLC controller and pump with a 2998 photodiode array detector using SunFire Prep C18 OBD (150 × 19 mm, 5 µm; Waters, Milford, MA, USA). The mobile phase consisted of water containing 0.1% (*v/v*) formic acid (A) and methanol (B), and was applied in linear gradient mode from 100% to 93% A at a flow rate of 7.0 mL/min for 40 min to yield uridine (**1**, 19.9 mg), adenosine (**2**, 28.1 mg), and guanosine (**3**, 12.0 mg). Nuclear magnetic resonance (NMR) data were obtained using a Varian VNMRS600 spectrophotometer (Varian, Palo Alto, CA, USA). LC-MS was performed using an Agilent 1260 Infinity system combined with an Agilent 6120 quadruple LC-MS system in positive ESI mode (Agilent Technologies, Santa Clara, CA, USA) with the following parameters: capillary voltage, 3.0 kV; nebulizer (N_2) pressure, 35 psi; drying gas temperature, 250 °C; drying gas flow, 12.0 L/min.

Uridine (**1**): ^{1}H NMR (600 MHz, D_2O) δ 7.87 (1H, d, *J* = 8.4 Hz, H-6), 5.91 (1H, d, *J* = 4.8 Hz, H-1′), 5.89 (1H, d, *J* = 8.4 Hz, H-5), 4.34 (1H, t, *J* = 5.1 Hz, H-2′), 4.22 (1H, t, *J* = 5.4 Hz, H-3′), 4.13 (1H, m, H-4′), 3.91 (1H, dd, *J* = 12.9, 2.7 Hz, H-5′), 3.80 (1H, dd, *J* = 12.9, 4.5 Hz, H-5′); ^{13}C NMR(150 MHz, D_2O): 163.9 (C-4), 149.4 (C-2), 139.5 (C-6), 100.0 (C-5), 87.0 (C-1′), 81.9 (C-4′), 71.3 (C-2′), 67.1 (C-3′), 58.4 (C-5′); ESI-MS *m/z* 245.3 $[M + H]^+$.

Adenosine (**2**): ^{1}H NMR (600 MHz, D_2O) δ 8.17 (1H, s, H-8), 8.01 (1H, s, H-2), 5.86 (1H, d, *J* = 6.0 Hz, H-1′), 4.56 (1H, t, *J* = 5.4 Hz, H-2′), 4.25 (1H, dd, *J* = 5.1, 3.9 Hz, H-3′), 4.13 (1H, q, *J* = 3.9 Hz, H-4′), 3.75 (1H, dd, *J* = 13.0, 2.7 Hz, H-5′), 3.66 (1H, dd, *J* = 13.0, 3.9 Hz, H-5′); ^{13}C NMR (150 MHz, D_2O) δ 151.3 (C-6), 147.5 (C-2), 145.9 (C-4), 139.0 (C-8), 116.7 (C-5), 86.1 (C-1′), 83.4 (C-4′), 71.6 (C-2′), 68.2 (C-3′), 59.1 (C-5′); ESI-MS *m/z* 268.3 $[M + H]^+$.

Guanosine (**3**): ^{1}H NMR (600 MHz, DMSO-d_6) δ 7.93 (1H, s, H-8), 5.69 (1H, d, *J* = 6.0 Hz, H-1′), 4.39 (1H, t, *J* = 5.4 Hz, H-2′), 4.08 (1H, t, *J* = 4.5 Hz, H-3′), 3.86 (1H, q, *J* = 3.6 Hz, H-4′), 3.61 (1H, dd, *J* = 12.0, 4.2 Hz, H-5′), 3.52 (1H, dd, *J* = 12.0, 4.2 Hz, H-5′); ^{13}C NMR (150 MHz, DMSO-d_6) δ 156.9 (C-6), 153.8 (C-2), 151.4 (C-4), 135.6 (C-8), 116.7 (C-5) 86.4 (C-1′), 85.2 (C-4′), 73.7 (C-2′), 70.4 (C-3′), 61.4 (C-5′); ESI-MS *m/z* 284.3 $[M + H]^+$.

HPLC quantification of **1**–**3** in the callus extract was performed with a Waters HPLC system equipped with a Waters 1525 binary pump, Waters 2707 autosampler, and Waters 2998 photodiode array detector using Acclaim Polar Advantage II C18 (250 × 4.6 mm, 5 µm; Thermo Fisher Scientific). The eluent was as follows: 0.1% formic acid-water (A) and methanol (B), with 100%–95% of solvent A for 40 min at a flow rate of 1.0 mL/min under 254 nm. Each sample was injected in a volume of 10 µL. Total phenolic and flavonoid contents were determined, as described previously [36–38].

2.3. Antioxidant Activity of P. pyrifolia Callus Extract

2.3.1. DPPH Radical Scavenging Assay

The DPPH radical scavenging activity of the callus extract was examined according to the method of Brand-Williams et al. [39]. Briefly, 100 µL of aqueous solution of callus extract or ascorbic acid was mixed with 100 µL of DPPH in methanol (0.2 mM). The mixtures were then incubated in the dark for 30 min at 25 °C. The negative control and background test sample were prepared by adding 100 µL of DPPH solution to 100 µL of methanol and ascorbic acid solution or callus extract, respectively. The absorbance of the sample at 517 nm was then measured against a blank consisting of a mixture of 100 µL DPPH solution and 100 µL water. The radical scavenging activity was calculated using the following equation:

$$\text{Free radical scavenging activity (\%)} = [1 - (B - C)/A] \times 100 \quad (1)$$

where A is the absorbance at 517 nm of the negative control, B represents the absorbance of the test sample at 517 nm, and C is the absorbance of the background test sample at 517 nm.

2.3.2. ABTS Radical Scavenging Assay

The ABTS radical scavenging activity was evaluated using the method of Re et al. with minor modifications [40]. $ABTS^{\bullet+}$ solution was produced by mixing 7 mM ABTS with 2.45 mM potassium persulfate solution (1:1, *v/v*) at 25 °C in the dark for 12–16 h. Then, this solution was diluted with water to obtain an absorbance of 0.70 ± 0.05 at 734 nm and used as a negative control. An aliquot of 100 µL of the test sample solution was mixed with 3.9 mL of the diluted $ABTS^{\bullet+}$ solution. After incubation at room temperature for 30 min, the absorbance of the mixture was measured at 734 nm. The ABTS radical scavenging activity was calculated using Equation (1) with C as the absorbance of the test sample at 734 nm before incubation.

2.3.3. FRAP Assay

The FRAP assay is a method for measuring the ability of antioxidants to reduce Fe^{3+} to Fe^{2+}, resulting in the formation of a blue-colored complex of Fe^{2+} with TPTZ, which shows absorbance at 593 nm. The assay was carried out based on the method described by Pulido et al. with some modifications [41]. The FRAP reagent was prepared by mixing 2.5 mL of TPTZ solution (10 mM TPTZ in 40 mM HCl), 2.5 mL of $FeCl_3$ solution (20 mM), and 45 mL of acetate buffer (300 mM at pH 3.6). Then, 3 mL of FRAP reagent was added to 100 µL of the sample solution. The mixture was incubated at 37 °C for 10 min, and the absorbance was measured at 593 nm relative to a blank (sample solution containing water instead of the callus extract). The antioxidant potential of the sample was determined based on a calibration curve prepared using $FeSO_4$ at concentrations of 0–2000 µM.

2.3.4. Protein Glycation Assay

The antiglycation effects of *P. pyrifolia* callus extract on collagen and elastin were evaluated using collagen and elastin glycation assay kits (Cosmo Bio Co., Ltd., Tokyo, Japan) according to the procedure described by the manufacturer. Briefly, all samples and standard solutions were kept at room temperature before analysis. For collagen glycation assay, 50 µL of collagen solution was aliquoted into 96-well black plates and incubated at 37 °C overnight to allow for gelation of the solution. To each well containing collagen gel was added 40 µL of different concentrations of aminoguanidine (antiglycation standard) or *P. pyrifolia* extract powder diluted in dilution buffer. Separately, elastin solution (50 µL) was added to each well of 96-well black plates followed by 40 µL of antiglycation standards and *P. pyrifolia* extract solution in dilution buffer. Then, glyceraldehyde solution (500 mM, 10 µL) was thoroughly mixed with each standard and sample in the wells, except for the sample blank. After immediately measuring fluorescence at 0 h using a fluorescence plate reader at an excitation wavelength of 370 nm and an emission wavelength of 440 nm, the plates were incubated at 37 °C for 24 h or 6 days under conditions of high humidity to induce collagen and elastin glycation, respectively. The formation of glycated collagen or elastin was then assessed by measuring the intensity of AGE-specific fluorescence. The inhibitory effect of glycation was calculated using the following equation based on the reduction of fluorescence intensity:

$$\text{Inhibition of protein glycation (\%)} = (B - A)/A \times 100 \quad (2)$$

where A represents the reduction in fluorescence intensity of the test sample before and after incubation, and B is the reduction in fluorescence intensity of the standard with 0 mM aminoguanidine before and after incubation.

2.4. Antiaging Potential of a Callus Extract of P. pyrifolia

2.4.1. Cell Proliferation Assay

In order to evaluate the effects of *P. pyrifolia* callus extract on keratinocyte (HaCaT) and fibroblast (CCD-986sk) cell proliferation, HaCaT or CCD-986sk cells were seeded at a density of 1×10^3 or 5×10^3 cells per well in 100 μL of Dulbecco's modified Eagle's medium (DMEM; Lonza, Zurich, Switzerland) containing 10% (*v/v*) fetal bovine serum (FBS; Thermo Fisher Scientific) and 1% (*v/v*) penicillin/streptomycin (Thermo Fisher Scientific) in each 96-well plate, and then incubated at 37 °C for 24 h. Next, the cells were treated with different concentrations of adenosine or *P. pyrifolia* callus extract in DMEM with 0.5% (*v/v*) FBS, alone or in combination, and incubated for a further 24 h. Cell viability was then evaluated by WST-1 assay (Roche Diagnostics, Mannheim, Germany) performed in accordance with the manufacturer's instructions. Briefly, 10 μL of diluted WST-1 solution (5 mg/mL in phosphate-buffered saline [PBS], pH 7.4) was added to each well and incubated for 2 h. The absorbance was then measured at 450 nm and the percentage cell viability was calculated by comparing the values of treated cells to those of untreated cells.

2.4.2. Procollagen Synthesis Assay

To determine whether the callus extract exerted antiwrinkle activity by promoting collagen production, the concentration of procollagen type I C-peptide synthesized by fibroblast cells was evaluated as a biomarker of procollagen formation. Aliquots of 1×10^4 CCD-986sk cells in 100 μL of DMEM with 10% (*v/v*) FBS were seeded into each well of 96-well plates and then cultured until the cells reached 80% confluence. After incubation in DMEM with 0.5% (*v/v*) FBS for 12 h, the cells were cultured in serum-free DMEM at 37 °C in the presence of various concentrations of callus extract alone or in combination with 0.015 μM of adenosine for a further 24 h. Next, the level of procollagen type I C-peptide in the culture medium was assessed using an enzyme-linked immunosorbent assay (ELISA) kit (Takara Bio, Shiga, Japan) according to the manufacturer's instructions.

2.4.3. In Vitro Scratch Wound Recovery Assay

To examine the promotion of skin regeneration by *P. pyrifolia* callus extract, HaCaT and CCD-986sk cells were seeded in Essen ImageLock 96-well plates (Essen Bioscience, Ann Arbor, MI, USA) at a density of 1×10^4 cells/well and 4×10^4 cells/well, respectively, and then cultured in complete medium at 37 °C for 48 h to form confluent monolayers. After treating the cells with 5 μg/mL mitomycin C in culture medium for 1 h to block proliferation, a scratched wound area (cell-free zone) was formed in each well using a wound-maker. The cells were then washed twice with PBS (pH 7.4) and further incubated in 200 μL of DMEM with 0.5% (*v/v*) FBS and different concentrations of adenosine or *P. pyrifolia* callus extract alone or in combinations at 37 °C. Wound closure induced by cell migration was observed every 6 h using an IncuCyte Zoom microscope (Essen Bioscience) and the extent of wound recovery was automatically calculated using phase-contrast image analysis software.

2.5. Preparation and Characterization of P. pyrifolia Callus Extract-Loaded NLs

P. pyrifolia callus extract-loaded NLs (PC-NLs) were produced by emulsification followed by microfluidization. Briefly, Lipoid P75-3 (2.5 g), Lipoid P100-3 (2.5 g), cholesterol (1 g), squalene (1 g), ethanol (1 g), and caprylic capryl triglyceride were mixed at 60 °C to form an oil phase. Separately, the *P. pyrifolia* callus extract (3 g) and glycerol (50 g) were dissolved in 34 g of water (aqueous phase). The oil phase was then slowly added to the aqueous solution and mixed at 3000 rpm for 10 min using a homogenizer (Primix Corp., Hyogo, Japan) to form a primary emulsion. Then, the primary emulsion was passed through a microfluidizer (LM20; Microfluidics Corp., Westwood, MA, USA) operating at 1000 bar (15 cycles) to prepare PC-NLs.

Callus extract-loaded elastic NLs (PC-ENLs) were produced by the thin-film hydration method followed by microfluidization. Briefly, the organic phase containing Lipoid P75-3 (4.28 g), Lipoid

P100-3 (4.28 g), and cholesterol (5.7 g) was dissolved in a mixture of chloroform and ethanol (4:1, *v/v*). Then, the organic solvent was completely removed using a rotary evaporator, forming a thin film in a round-bottomed flask. The aqueous phase containing the callus extract (1.85 g) and Tween 80 (1.07 g) in 11.14 mL of PBS (pH 7.4) was added to the flask, followed by hydration of the thin film with continuous sonication. After adding 33.42 mL of PBS (pH 7.4), the dispersion was then passed through a microfluidizer at a pressure of 1000 bar for 15 cycles to form nanosized elastic NLs containing callus extract.

To evaluate the average encapsulation efficiency of *P. pyrifolia* callus extract in NLs or elastic NLs, 500 μL of the dispersion of NLs was centrifuged at 18,000 rpm for 1 h. The concentration of unincorporated adenosine in the supernatant was then determined by HPLC at 320 nm, as described above. In addition, the mean hydrodynamic diameter, polydispersity index (PDI), and zeta potential of the PC-NLs or PC-ENLs were assessed at 25 °C by dynamic light scattering (Malvern Zetasizer Nano ZS90; Malvern Instruments, Malvern, UK) after dilution in deionized water (1:20). The NLs were further diluted 1:100 in water, and drops of the diluted NLs were placed on copper grids. After removing excess liquid with filter paper, a drop of 2% (*w/v*) aqueous phosphotungstic acid was added to the grid for negative staining and the morphology of the NLs was examined by transmission electron microscopy (TEM, JEM-200; JEOL, Tokyo, Japan).

2.6. In Vitro Skin Permeability of P. pyrifolia Callus Extract-Loaded NLs

The in vitro artificial skin permeabilities of *P. pyrifolia* callus extract, PC-NLs, or PC-ENLs were evaluated using a Skin PAMPA Explorer Test System (Pion, Billerica, MA, USA). Each well of the top (donor) compartment of a Skin PAMPA sandwich plate was hydrated with 200 μL of diluted hydration solution (pH 7.4) overnight. Before forming the sandwich, the bottom (acceptor) plate was filled with 200 μL of Prisma-HT buffer solution (pH 7.4). Then, 200 μL of each sample solution of *P. pyrifolia* callus extract, PC-NLs, or PC-ENLs diluted with Prisma-HT buffer solution (equivalent to 100 μg/mL adenosine) was loaded into the donor plate well and the resulting sandwich was incubated at room temperature. After 1, 3, 6, 9, 12, and 24 h, each PAMPA sandwich was separated, and 100 μL aliquots of both donor and acceptor solutions were collected. The adenosine from the permeated *P. pyrifolia* callus extract in the artificial skin permeation experiments was quantified using an HPLC system with UV detection, as described above.

To evaluate the human skin permeability of the *P. pyrifolia* callus extract or PC-ENLs across an epidermal layer, human epidermis (Huskin; Hans Biomed Corp., Daejeon, Republic of Korea) was mounted with the SC facing upward on the receptor compartment of a Franz diffusion cell system containing 5 mL of PBS (pH 7.4). After the donor compartment was clamped in place, 500 μL of *P. pyrifolia* callus extract or PC-ENLs diluted in PBS (pH 7.4) (equivalent to 100 μg/mL adenosine) was loaded into the donor compartment (diffusion area: 0.785 cm^2). The receptor compartments were stirred at 600 rpm and skin surfaces were maintained at 32 °C during the experiment. At 1, 3, 6, 9, 12, and 24 h after loading of the sample solutions, 200 μL of the receptor phase solution was withdrawn and filled with 200 μL of fresh PBS (pH 7.4). After filtering the samples through polyvinylidene difluoride (PVDF) membrane filters (pore size: 0.45 μm), permeated adenosine from the callus extract or PC-ENLs was assessed by HPLC at 254 nm, as described above.

2.7. Statistics

The *t* test was used to compare two mean values of unpaired data, and one-way analysis of variance (ANOVA) followed by Tukey's multiple comparison test was used to compare three or more mean values of unpaired data. All data are expressed as means ± standard deviation, and $p < 0.05$ was taken to indicate statistical significance.

3. Results and Discussion

3.1. Preparation and Characterization of Callus Extract from P. pyrifolia

The pale yellowish *P. pyrifolia* callus was successfully induced after transferring in vitro-derived young leaf explants into M&S medium with 2.0 mg/L picloram in comparison with those in 2 mg/mL of 2,4-dichlorophenoxy-acetic acid and 6-benzylaminopurine alone or in combination. Furthermore, plant cell proliferation at the site of explant injury as well as in suspension was maximally stimulated using picloram as a growth regulator in medium supplemented with vitamins, including myoinositol, pyridoxine hydrochloride, nicotinic acid, thiamine hydrochloride, and riboflavin.

The aqueous extract derived from *P. pyrifolia* callus was screened using HPLC with a photodiode array detector (HPLC-PDA) to determine the chemical composition. Three compounds were detected and isolated from the extract, and their structures were identified unambiguously as uridine (**1**), adenosine (**2**), and guanosine (**3**) by spectroscopic analyses, including UV, NMR, and mass spectrometry, as well as by comparison with standards (Figure 1). The contents of nucleosides **1**–**3** in the extract were evaluated using calibration curves based on peak areas (Y) and concentrations (X, μg/mL) in the ranges of 10–1000 μg/mL. Each calibration curve showed good linear regression as follows: uridine (**1**), Y = 19,494X − 19,998, r^2 = 1.0000; adenosine (**2**), Y = 25,897X – 41,736, r^2 = 1.0000; guanosine (**3**), Y = 25,009X − 8108.2, r^2 = 1.0000. Therefore, the contents of the three ribonucleosides in the callus extract were determined to be 1620.15 ± 2.28 (**1**), 1961.55 ± 6.98 (**2**), and 1088.97 ± 2.08 (**3**) μg/g.

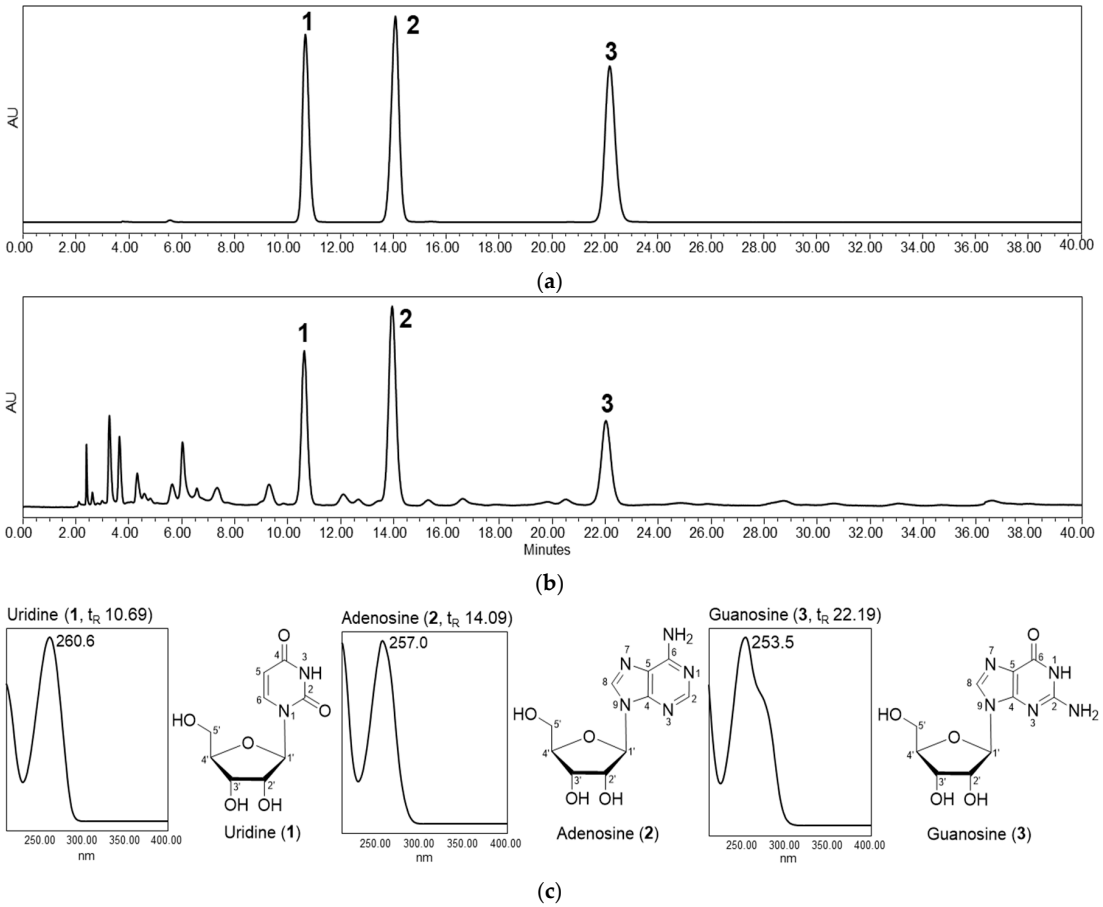

Figure 1. High-performance liquid chromatography (HPLC) profiles and chemical structures of the major compounds in *Pyrus pyrifolia* callus extract. (**a**) HPLC chromatograms of three standards, uridine (**1**), adenosine (**2**), and guanosine (**3**), and (**b**) aqueous extract from *P. pyrifolia* callus at 254 nm. (**c**) Structures of compounds and their ultraviolet (UV) spectra obtained with a photodiode array detector (210–400 nm).

Pyrimidine nucleoside uridine has been shown to rapidly restore the ocular surface in patients with dry eye by increasing hyaluronic acid synthesis, reducing degradative enzymes, such as matrix metalloproteinase-9, and enhancing the number of goblet cells [42]. Adenosine is a naturally occurring purine nucleoside formed by the breakdown of adenosine triphosphate, which is a member of an important class of bioactive molecules with antiwrinkle properties [43]. Therefore, adenosine has been applied in cosmetic preparations to improve facial wrinkles. The guanine-based purine, guanosine, exhibits beneficial effects on injured neural cells and can modulate several signaling pathways to provide neuroprotection. Furthermore, it can modulate glutamatergic metabolism, avoiding overactivation of glutamate receptors, and exerting antioxidant and anti-inflammatory activities [44]. Therefore, the callus extract was expected to possess biological activities related to skin regeneration.

Phytochemicals, such as phenolic and flavonoid compounds, have been reported to possess significant antioxidant properties, which are crucial for antiaging skin care products conferring protection against UV radiation and inflammation [45]. However, the total content of phenolic compounds in the callus extract was 9.25 ± 0.14 mg/g of gallic acid equivalents, and flavonoids were not detected by the corresponding $AlCl_3$ method, which has lower sensitivity for phenolics and flavonoids than the levels in the extracts of *P. pyrifolia* peel or flesh. In addition, the presence of major phenolics and flavonoids in the *P. pyrifolia* callus extract could not be clearly determined by HPLC-PDA experiments. This may have been due to environmental factors related to the light/dark incubation of callus and the level of picloram in M&S culture medium. Previous studies indicated that the production of phenolics was hindered when the callus was induced under dark conditions, and thereafter the total contents of phenolics and flavonoids were lower than those in the in vivo-derived plant extract [46]. Therefore, the light/dark incubation of cultures may play an important role in phenolic accumulation. Moreover, higher levels of picloram in the culture medium and extraction under aqueous conditions can reduce the total phenolic and flavonoid levels in the in vitro plant extract, which would further influence the antioxidant potential [31].

3.2. Antioxidant Activities of P. pyrifolia Callus Extract

3.2.1. Antioxidant Activities of *P. pyrifolia* Callus Extract

The antioxidant activity of the *P. pyrifolia* callus extract was expressed as the ability to scavenge free radicals in DPPH and ABTS assays, and to reduce ferric ions in the FRAP test, because radical scavenging activities in the extracts of many plants, vegetables, and fruits have been reported to be linearly correlated with the total phenolic compound and total flavonoid contents [47]. As shown in Figure 2, the callus extract and ascorbic acid (positive control) exhibited dose-dependent radical scavenging activity. In the DPPH assay, the callus extract showed free radical scavenging activity of 76.9% ± 2.88% at 300 μg/mL, which was comparable to that of 44 μg/mL ascorbic acid (82.5% ± 3.63%). The IC_{50} value of the callus extract was 124 ± 6.64 μg/mL, which was equivalent to the value of 16.8 ± 1.81 μg/mL for ascorbic acid (Figure 2a). However, the IC_{50} of the callus extract in the ABTS test was 1236 ± 7.122 μg/mL, which was 6.84 times higher than that of ascorbic acid (181 ± 0.491 μg/mL) (Figure 2b). The observed differences in the capacity of the callus extract to scavenge ABTS and DPPH radicals may have been mainly because, in these assays, the transfer of hydrogen and the transfer of electrons occur at different redox potentials and are dependent on the structures of the antioxidants [48]. The callus extract also showed dose-dependent ferric reducing power in the FRAP assay, which was based on the ability to reduce Fe^{3+} to Fe^{2+}. At 300 μg/mL, the callus extract exhibited ferric reducing activity of 46.8% ± 3.02%, which was comparable to the value of 719 ± 61.8 μmoL Fe(II)/g for deionized water.

The present findings obtained from three antioxidant assays (DPPH, ABTS, and FRAP) indicated that the callus extract had antioxidant properties related to the total phenolic content. However, antioxidant activity was lower than that reported previously for a pear extract; the DPPH and ABTS

free radical scavenging activities of the ethanol extract of pear peel were reported to be 78.4% ± 0.5% and 78.4% ± 1.1%, respectively, at a concentration of 100 μg/mL [49]. Therefore, further studies are required to optimize the callus culture conditions and solvent system for extraction to enhance the contents of secondary metabolites with potent antioxidant activity.

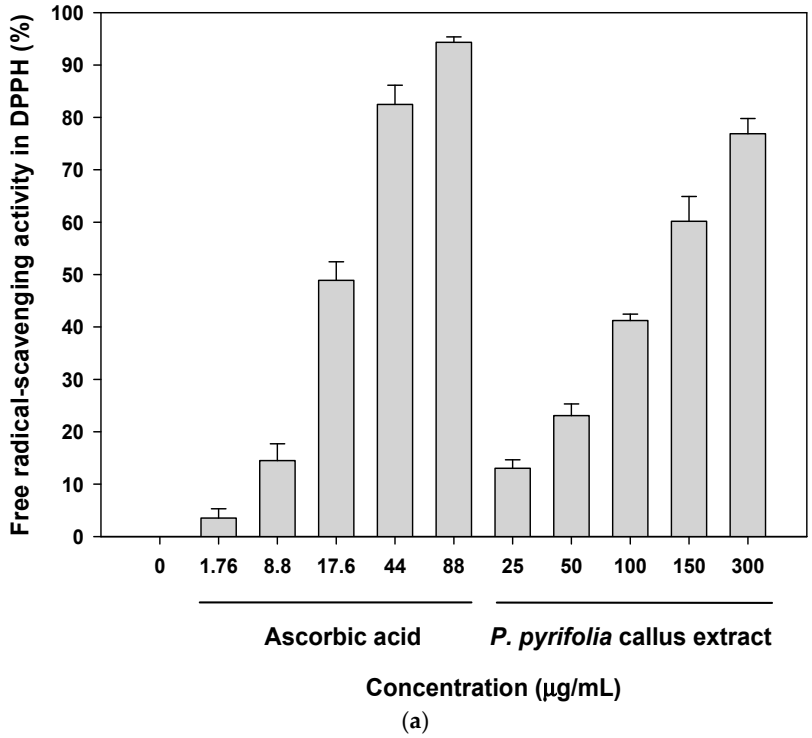

(**a**)

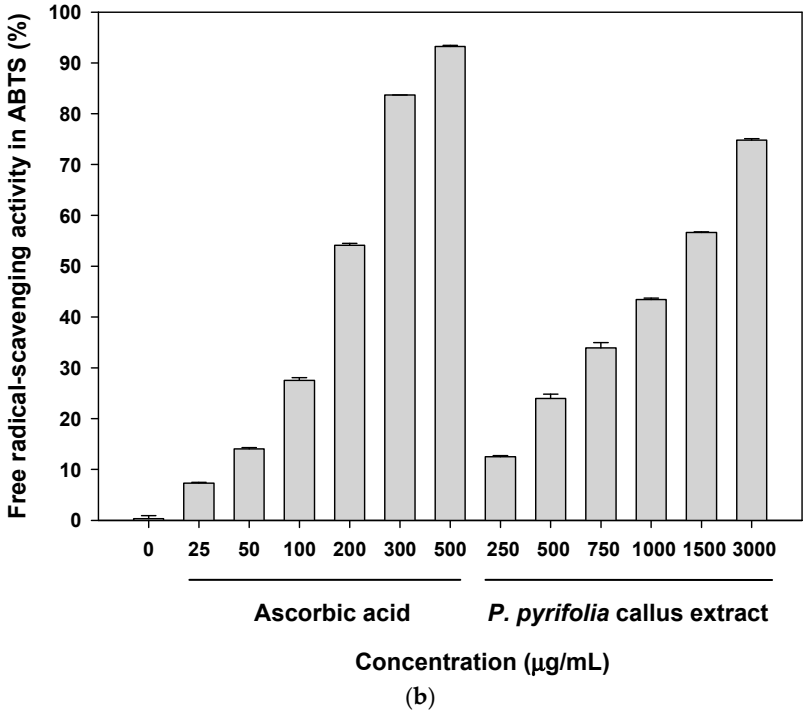

(**b**)

Figure 2. Antioxidant activity of the aqueous extract of *P. pyrifolia* callus. (**a**) 2,2-Diphenyl-2-picrylhydrazyl (DPPH) and (**b**) 2,2′-azinobis-(3-ethylbenzoline-6-sulfonate) (ABTS) free radical scavenging activity. Values are the means ± standard deviation (n = 6 per group).

3.2.2. Antiglycation Potential of *P. pyrifolia* Callus Extract

Glycation of protein components of the ECM in the dermis severely damages skin elasticity by cross-linking the fibers, thereby reducing their elasticity. Non-cross-linked advanced glycation end products (AGEs), such as N^{ε}-(carboxymethyl) lysine (CML), also accumulate in the epidermis as well as in collagen. The age-related accumulation of CML results in reduced skin elasticity and the development of a dull appearance and lack of firmness of the skin [50]. To evaluate the inhibitory activities of *P. pyrifolia* callus extract on collagen and elastin glycation, we measured the total fluorescent AGEs in collagen or elastin glycated with glyceraldehyde. As shown in Figure 3a, aminoguanidine, one of the most promising pharmacological interventions for inhibiting glycation, exhibited 45.7% ± 2.24% inhibition of AGE formation in collagen at 741 μg/mL, with an IC_{50} of 727 ± 49.9 μg/mL. The callus extract also inhibited the glycation of collagen in a dose-dependent manner; at 5000 μg/mL, the callus extract exhibited 89.3% ± 2.70% inhibition of AGE formation in collagen. In addition, after treatment with 3000 μg/mL of the callus extract, the magnitude of the collagen glycation inhibitory effect was 47.8% ± 3.18%, which was equivalent to that of 741 μg/mL aminoguanidine.

Figure 3b shows the effect of *P. pyrifolia* callus extract on total AGE formation in elastin over a 6-day incubation period. The fluorescence intensity of elastin incubated with glyceraldehyde increased significantly by about nine-fold in comparison to that of elastin alone, indicating progressive formation of AGEs. When elastin glycation occurred in the presence of 741 μg/mL aminoguanidine, the percentage inhibition of AGE formation was 57.4% ± 0.451%, with an estimated IC_{50} value of 602 ± 2.72 μg/mL. The callus extract also significantly reduced the formation of AGEs in a concentration-dependent manner, and at 5000 μg/mL, the callus extract decreased AGE formation by 82.7% ± 4.59%. Upon incubation of elastin with glyceraldehyde and 3000 μg/mL callus extract, the percentage inhibition of AGE formation was 51.3% ± 1.45%, which was comparable to the effect of 741 μg/mL aminoguanidine.

Although the level of phenolic compounds in callus extract was low, positive glycation inhibitory effects on collagen and elastin, which have crucial roles in maintaining the structural integrity and elasticity of the skin, were observed. However, further cell-based antioxidant studies are required to examine the possible antiaging effect of the callus extract on the skin via its inhibition of ROS-induced oxidative damage to cells, which leads to lipid peroxide formation, mitochondrial and DNA damage, and alterations in protein and gene function [9].

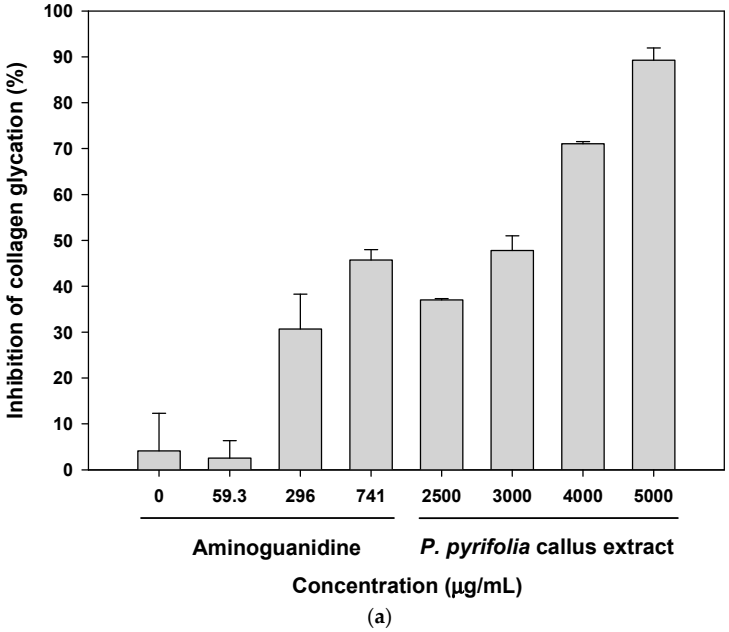

(**a**)

Figure 3. *Cont.*

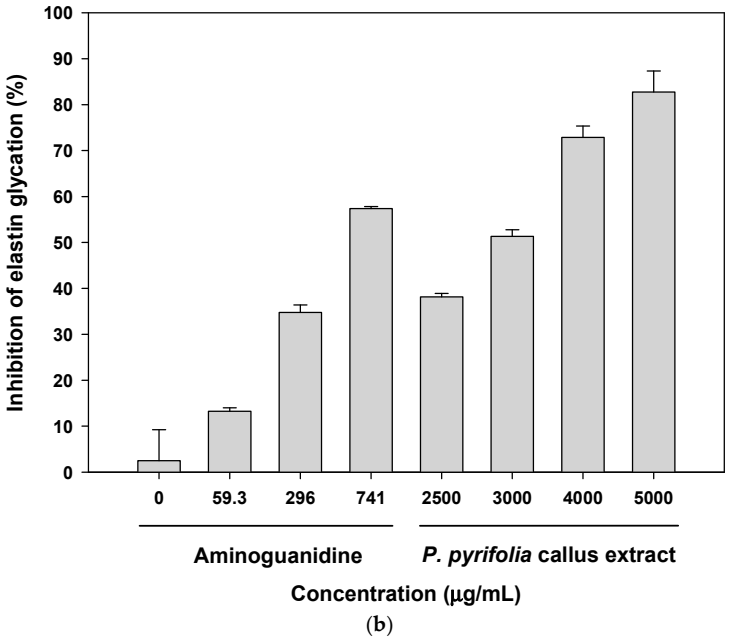

(**b**)

Figure 3. In vitro antiglycation effects of *P. pyrifolia* callus extract. Inhibition of advanced glycation end product (AGE) formation in (**a**) collagen and (**b**) elastin via glyceraldehyde in the absence or presence of the indicated concentrations of aminoguanidine or callus extract. Data are the means ± standard deviation percentages of the control (n = 6 per group).

3.3. Skin Regeneration Activities of P. pyrifolia Callus Extract

3.3.1. Effects of Callus Extract and Combination of Callus Extract and Adenosine on Keratinocyte and Fibroblast Cell Proliferation

In vitro cell viability assays were performed using HaCaT and CCD-986sk cells to determine the effects of *P. pyrifolia* callus extract alone and in combination with adenosine on cell proliferation. As shown in Figure 4a, adenosine and *P. pyrifolia* callus extract exhibited dose-dependent stimulation of HaCaT cell proliferation; 0.015 μM adenosine significantly increased cell proliferation by 110% ± 2.51% and cells treated with 15 μM adenosine showed 49% more proliferation than the controls. The relative proliferation of cells treated with 1.36 μg/mL *P. pyrifolia* callus extract was 123% ± 3.68%, which was equivalent to that of cells treated with 1.5 μM adenosine (124% ± 3.71%). At 13.6 μg/mL, *P. pyrifolia* callus extract induced a 31% increase in HaCaT cell proliferation compared to controls, indicating that *P. pyrifolia* callus extract alone effectively stimulated HaCaT cell growth. Cells treated simultaneously with adenosine (0.015 μM) and *P. pyrifolia* callus extract (0.0136 μg/mL) showed significantly increased proliferation (172% ± 12.6%), which was 1.28- and 1.87-fold higher than those seen with adenosine and *P. pyrifolia* callus extract alone, respectively (Figure 4b).

Similarly, the proliferation of CCD-986sk cells also increased with increasing adenosine concentration, and the relative cell proliferation at 15 μM adenosine was 70% higher than that of controls. On the other hand, fibroblast cell growth was increased to 156% ± 5.42% at 0.0136 μg/mL of *P. pyrifolia* callus extract, which was 11% higher than that seen with 0.15 μM adenosine, but cell proliferation was not significantly increased at *P. pyrifolia* callus extract concentrations >0.0136 μg/mL (Figure 4c). Combined treatment with adenosine and *P. pyrifolia* callus extract also resulted in a greater cell proliferative effect than either agent alone (Figure 4d). Additionally, the proliferation of human fibroblasts was maximized by treatment with 0.0136 μg/mL of *P. pyrifolia* callus extract combined with 0.015 μM adenosine, and the relative cell proliferation was 12% and 5% greater than those seen with adenosine (0.015 μM) or *P. pyrifolia* callus extract (0.0136 μg/mL), respectively.

The strong cell proliferation activity of *P. pyrifolia* callus extract on keratinocytes and fibroblasts may be closely related to the presence of uridine (**1**), adenosine (**2**), and guanosine (**3**), suggesting that the callus extract may be a potent rejuvenator when included along with other antiaging ingredients, such as adenosine, in cosmetic formulations to improve undesirable wrinkles.

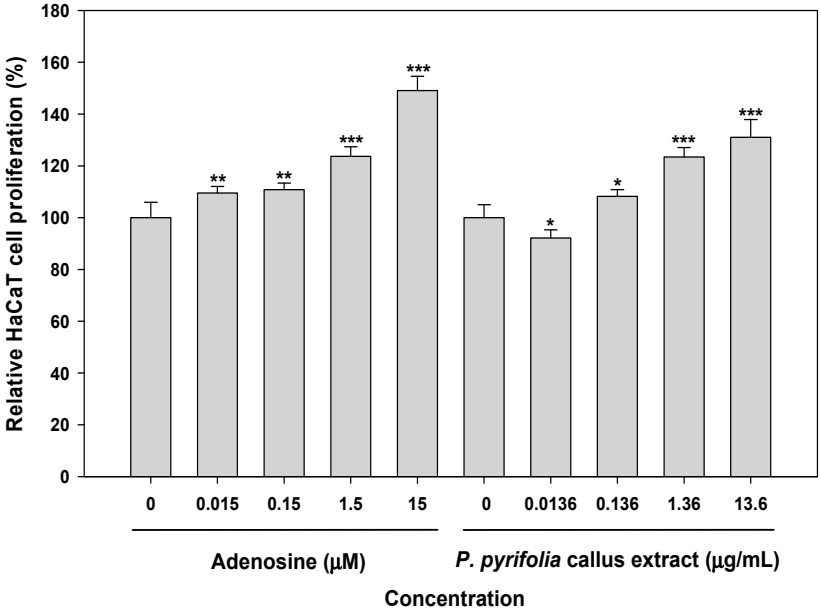

(**a**)

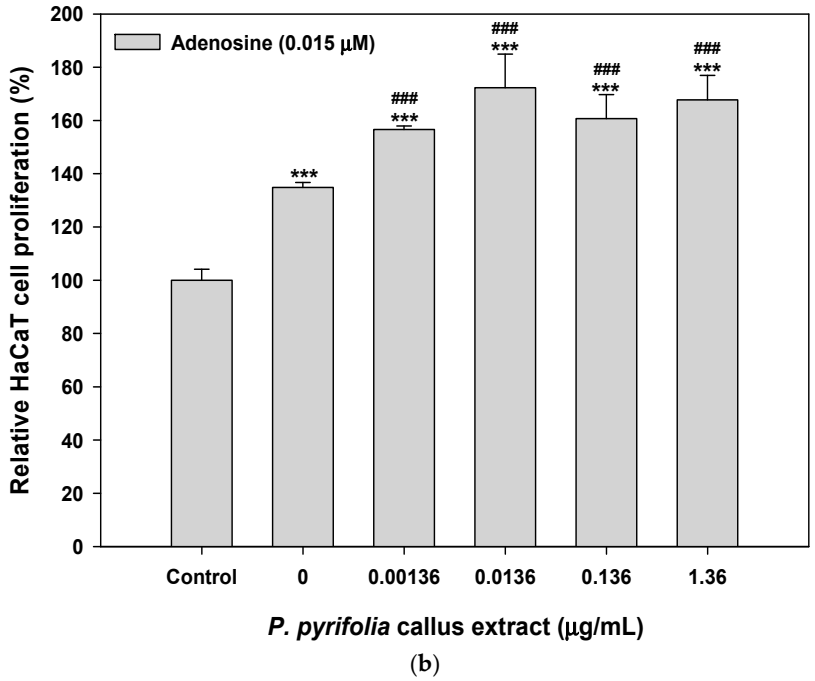

(**b**)

Figure 4. *Cont.*

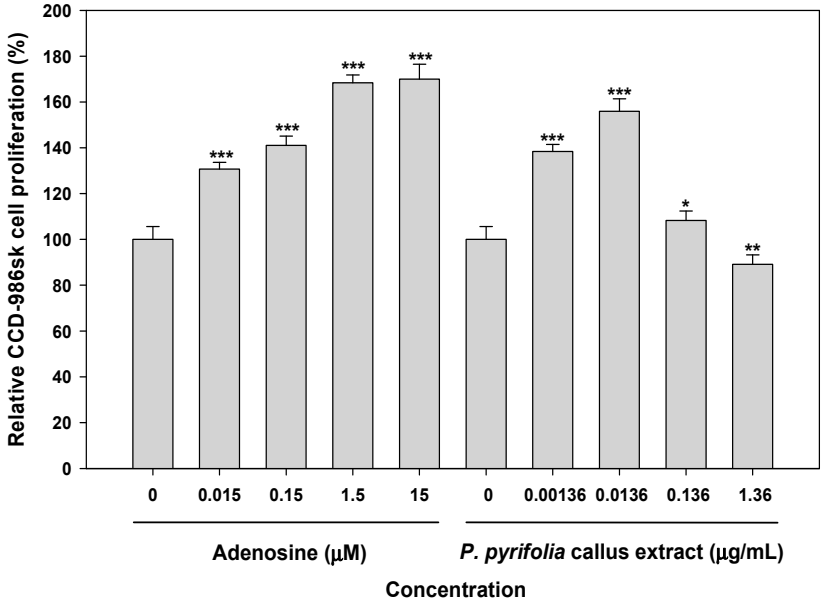

(**c**)

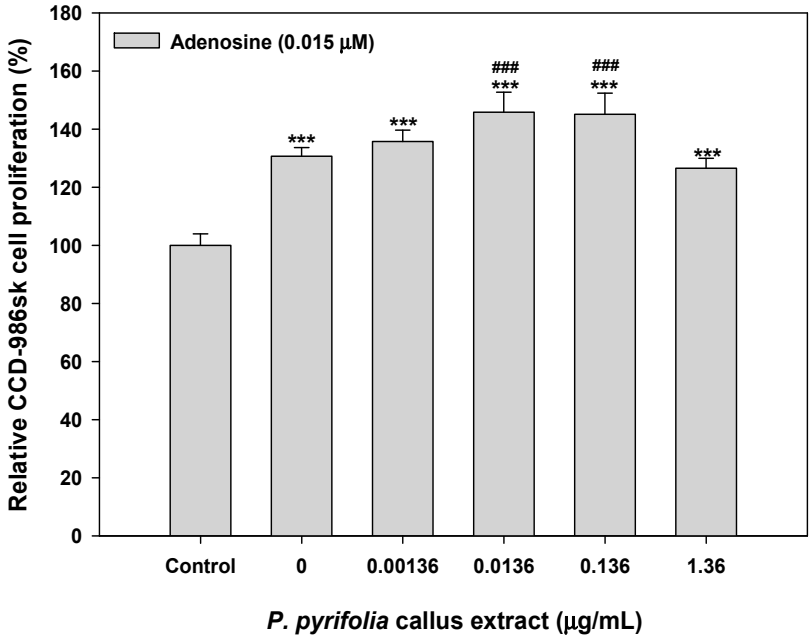

(**d**)

Figure 4. Relative HaCaT cell proliferation after treatment with (**a**) *P. pyrifolia* callus extract alone or (**b**) in combination with adenosine (0.015 μM). CCD-986sk cell proliferation after treatment with (**c**) *P. pyrifolia* callus extract alone or (**d**) in combination with adenosine (0.015 μM). Values are means ± standard deviation (n = 6 per group). * $p < 0.05$, ** $p < 0.01$, *** $p < 0.001$ compared to untreated controls. ### $p < 0.001$ compared to 0.015 μM adenosine alone.

3.3.2. Procollagen Synthesis Effects of Treatment with *P. pyrifolia* Callus Extract Alone and in Combination with Adenosine

Collagen, one of the major proteins in ECM, is the main building block of connective tissue, hair, and nails, and is responsible for maintaining the elasticity, strength, and flexibility of skin. In addition, adenosine has been shown to modulate cellular and organ function via occupancy of four specific cell surface receptors (A1, A2A, A2B, and A3), all of which are members of the large family of 7-transmembrane spanning and heterotrimeric G protein-associated receptors [51]. In particular,

the activation of adenosine A2A receptors promoted collagen synthesis of human fibroblast cells [52]. Therefore, topical treatment with adenosine increased the number of myofibroblasts, which are responsible for the contraction of granulation tissue during tissue regeneration, with increasing concentration. Therefore, we examined the effects of callus extract alone or in combination with adenosine on collagen production by human fibroblasts by measuring the level of procollagen type I C-peptide. As shown in Figure 5, the biosynthesis of procollagen type I C-peptide by CCD-986sk cells was promoted by the extract in a dose-dependent manner and significantly increased by treatment with 0.0136–1.36 μg/mL of *P. pyrifolia* callus extract in comparison with the control group; cells treated with 1.36 μg/mL of *P. pyrifolia* callus extract showed 1.60- and 1.43-fold increases in the levels of procollagen type I C-peptide, respectively, compared to control cells and those treated with adenosine alone (0.015 μM). In addition, the synthesis of procollagen type I C-peptide was enhanced by adding *P. pyrifolia* callus extract to adenosine (0.015 μM); the level of procollagen type I C-peptide production after treatment with a combination of *P. pyrifolia* callus extract (0.0136 μg/mL) and adenosine (0.015 μM) was 1.51-, 1.11-, and 1.35-fold greater than after treatment with control, callus extract alone (0.0136 μg/mL), and adenosine alone (0.015 μM), respectively. These results confirmed the fibrogenic role of the callus extract alone and in combination with adenosine on the skin.

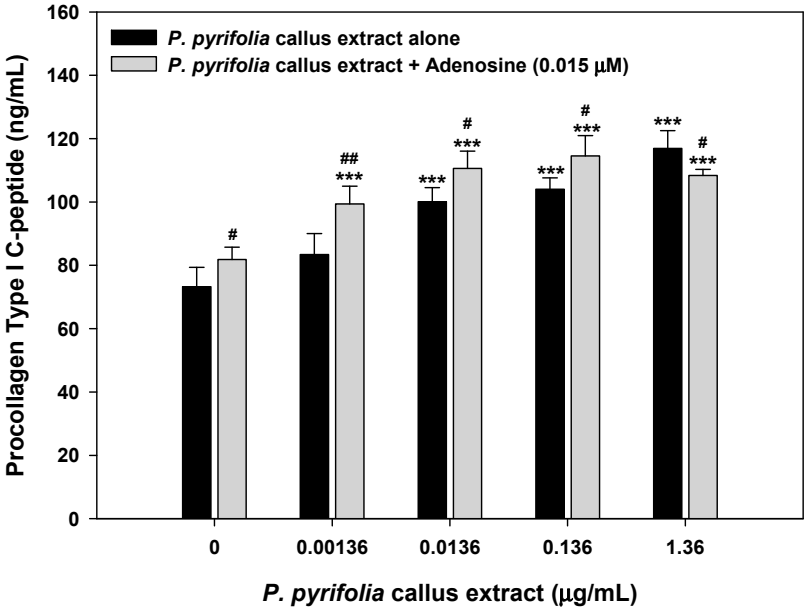

Figure 5. Procollagen type I C-peptide synthesis by CCD-986sk cells after treatment with *P. pyrifolia* callus extract alone or in combination with adenosine (0.015 μM) for 24 h. Values are means ± standard deviation ($n = 6$ per group). *** $p < 0.001$ compared to untreated control. # $p < 0.05$, ## $p < 0.01$ compared to the same concentration of *P. pyrifolia* callus extract alone.

3.3.3. Effects of *P. pyrifolia* Callus Extract Alone and in Combination with Adenosine on In Vitro Scratch Wound Recovery

Next, we examined the dose-dependent effects of *P. pyrifolia* callus extract alone and in combination with adenosine on HaCaT cell proliferation/migration using a wound healing assay. Both *P. pyrifolia* callus extract and adenosine alone promoted relative wound recovery in a dose- and time-dependent manner. Treatment with *P. pyrifolia* callus extract alone (1.36 μg/mL) for 9 h significantly accelerated wound closure of keratinocytes, with a value of 68.5% ± 2.18%, which was higher than those for control treatment and treatment with 0.15 μg/mL adenosine alone. Similarly, adenosine also induced a dose-dependent increase in HaCaT cell proliferation/migration up to 15 μM, and the relative wound recovery at 1.5 μM adenosine was equivalent to that of 1.36 μg/mL of callus extract (Figure 6a). The process of wound closure, driven by the proliferation/migration of HaCaT

cells, is illustrated by representative images in Figure 6b,c. The relative wound recovery at 9 h after the combined treatment with *P. pyrifolia* callus extract (0.0136 μg/mL) and adenosine (0.015 μM) was 72.8% ± 5.07%, which was 21% greater than those seen with the same concentrations of *P. pyrifolia* callus extract (60.0% ± 3.76%) or adenosine (60.4% ± 2.04%) alone (Figure 6b). Although the wounded area in the combined treatment group was recovered completely at 12 h (93.7% ± 5.46%), sizeable wound area gaps in the monolayer were still present in the control as well as in the cells treated with *P. pyrifolia* callus extract or adenosine alone. At 12 h after treatment with serum-free medium (control), *P. pyrifolia* callus extract, or adenosine, the relative wound recovery values were 85.2% ± 3.89%, 82.2% ± 4.37%, and 89.0% ± 5.89%, respectively.

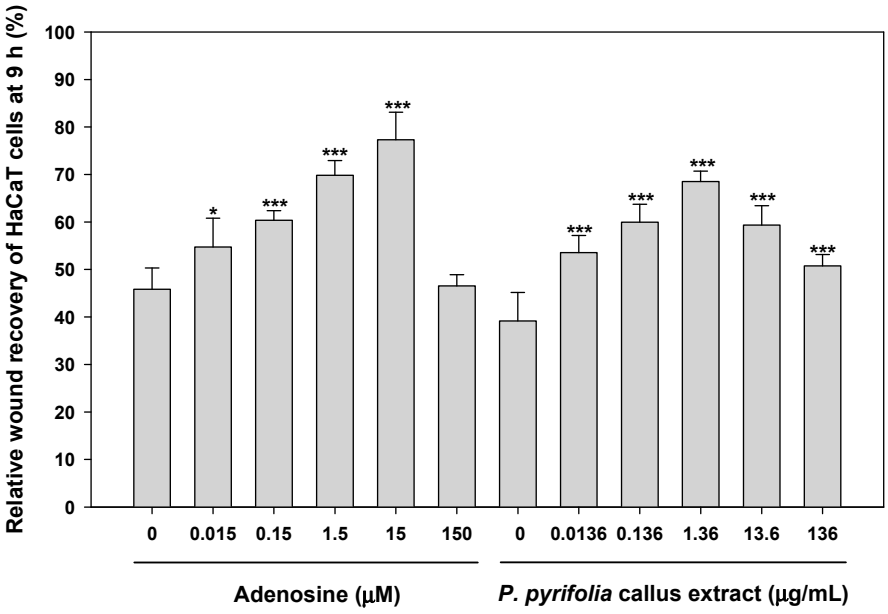

(**a**)

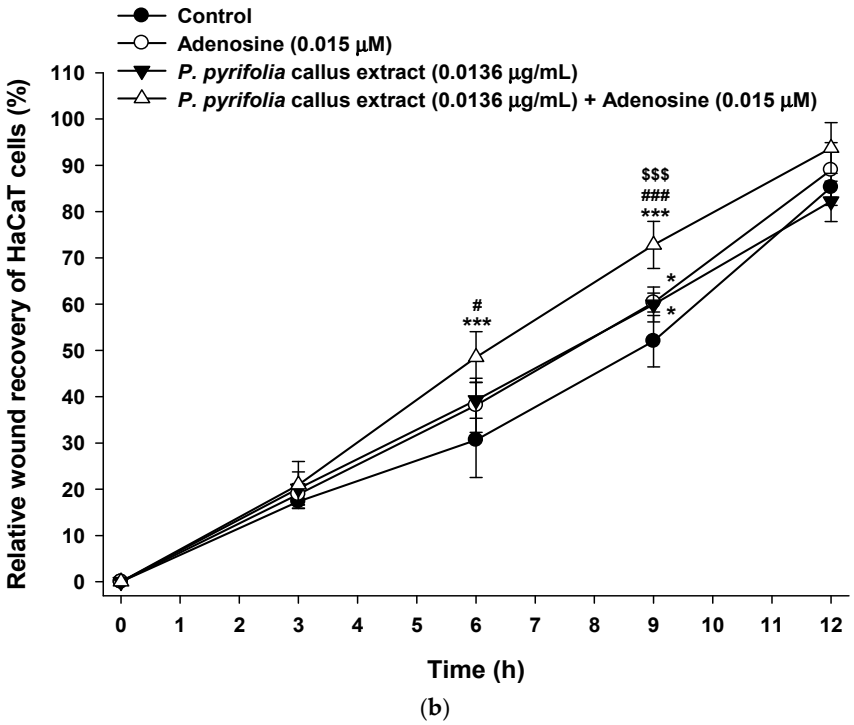

(**b**)

Figure 6. *Cont*.

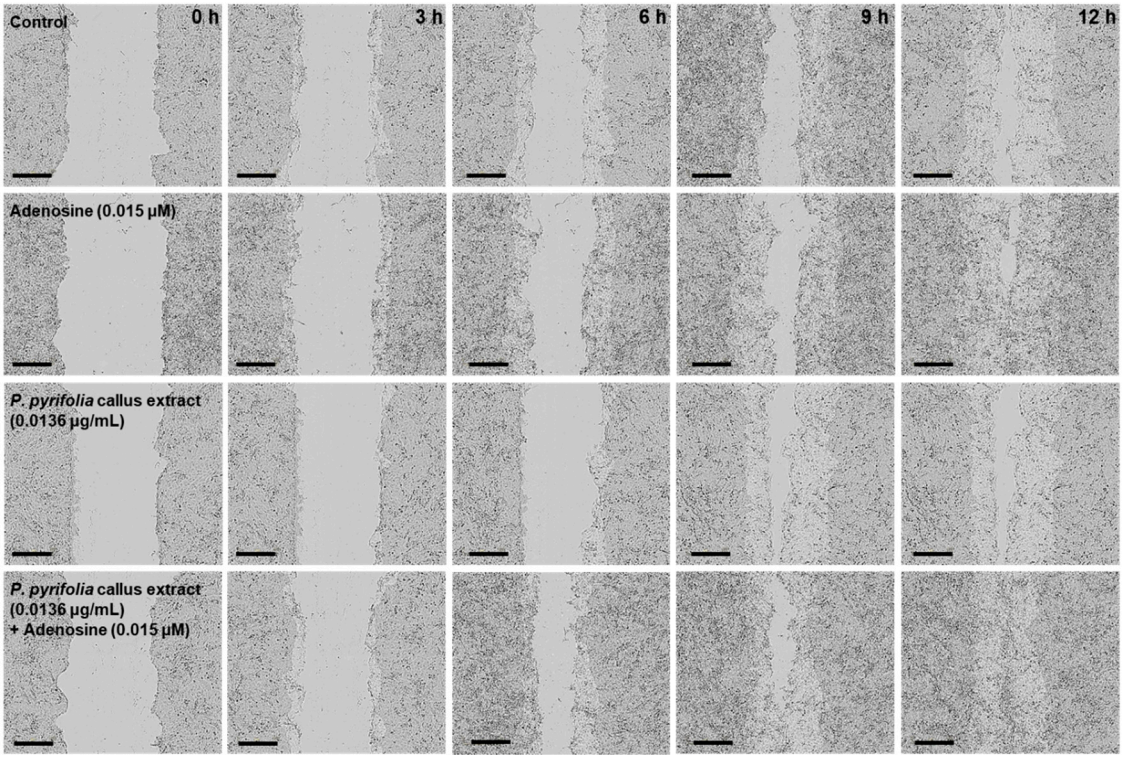

(**c**)

Figure 6. Relative scratch wound recovery of HaCaT cells after incubation with adenosine and *P. pyrifolia callus* extract. (**a**) Relative scratch wound recovery of HaCaT cells after 9 h. (**b**) Time course of relative scratch wound recovery area of HaCaT cells. (**c**) Representative microscopic images of scratch wounds after cells were treated with serum-free medium (control), adenosine (0.015 μM), and *P. pyrifolia* callus extract (0.0136 μg/mL) alone or in combination with adenosine (0.015 μM). Values are means ± standard deviation ($n = 6$). * $p < 0.05$, *** $p < 0.001$ compared to untreated control. # $p < 0.05$, ### $p < 0.001$ compared to adenosine alone (0.015 μM). $$$ $p < 0.001$ compared to *P. pyrifolia* callus extract alone (0.0136 μg/mL). Scale bar in (**c**): 300 μm.

In vitro scratch wound recovery assay with human fibroblast cells yielded similar results (Figure 7). Treatment of fibroblasts with *P. pyrifolia* callus extract or adenosine alone led to rapid scratch wound closure of CCD-986sk cell monolayers. Therefore, the recovery rates after 36 h of treatment with *P. pyrifolia* callus extract (0.0136 μg/mL) or adenosine (0.015 μM) alone were 22% and 33% higher than that of serum-free medium control (56.9 ± 7.31%), respectively (Figure 7a). In addition, at 36 h after treatment with 1.36 μg/mL of *P. pyrifolia* callus extract or 1.5 μM adenosine alone, the wound closure area had increased by 38% and 48% compared to the control group, respectively, but there were no obvious improvements in scratch wound recovery when the concentrations of callus extract or adenosine were increased above 1.36 μg/mL and 1.5 μM, respectively. In addition, combined treatment with *P. pyrifolia* callus extract (0.0136 μg/mL) and adenosine (0.015 μM) significantly accelerated wound closure in comparison to the control. A synergistic effect on wound closure was observed after treatment with *P. pyrifolia* callus extract (0.0136 μg/mL) along with adenosine (0.015 μM), and their wound recovery rates were maximally accelerated by 31% and 18% compared to each material alone, respectively, at 24 h after treatment (Figure 7b,c). Thus, almost complete wound closure at 48 h was observed with combined *P. pyrifolia* callus extract (0.0136 μg/mL) and adenosine (0.015 μM) treatment, resulting in relative wound recovery of 92.1% ± 3.14%, which was 1.20-, 1.08-, and 1.10-fold higher than the recovery rates of control cells or cells treated with the same concentrations of *P. pyrifolia* callus extract (85.2% ± 4.90%) and adenosine (84.0% ± 6.91%) alone, respectively.

The results presented here support the enhancement of skin regeneration by callus extract via its major bioactive nucleosides, including uridine, adenosine, and guanosine. Uridine ointment was reported to ameliorate 5-fluorouracil (FU)-induced skin toxicity as well as to protect against 5-FU-induced keratinocyte damage without influencing the anticancer efficacy of 5-FU [53]. In addition, adenosine A2A receptors are expressed on most cell types involved in wound healing, including macrophages, fibroblasts, and microvascular endothelial cells. Previous studies indicated that both adenosine A2A and A2B receptors contributed to enhanced fibroblast and endothelial cell migration [54]. Furthermore, adenosine can promote angiogenesis by inhibiting endothelial secretion of the antiangiogenic factor, thrombospondin-1, stimulating the production of vascular endothelial growth factor (VEGF) by macrophages via activation of adenosine A2A receptors, and inducing VEGF release by retinal endothelial cells through A2B receptors [51,55].

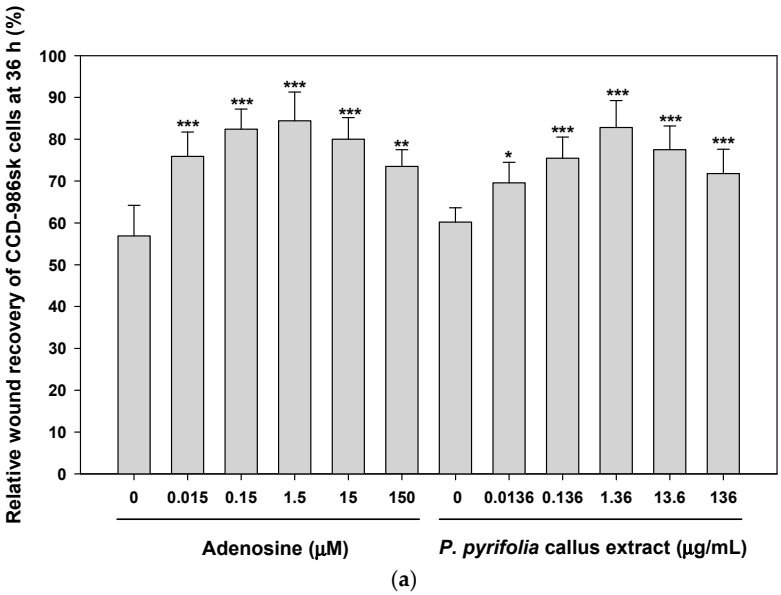

(**a**)

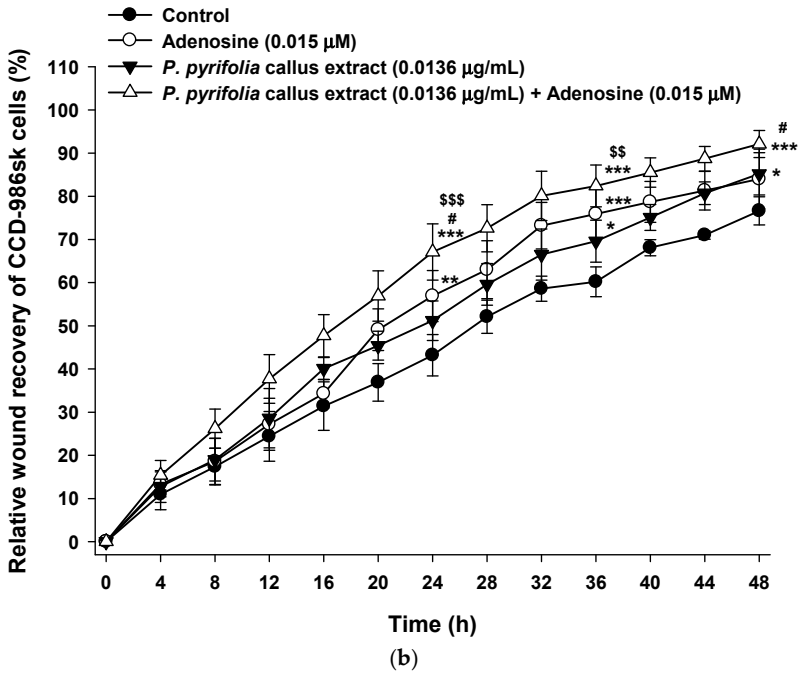

(**b**)

Figure 7. *Cont.*

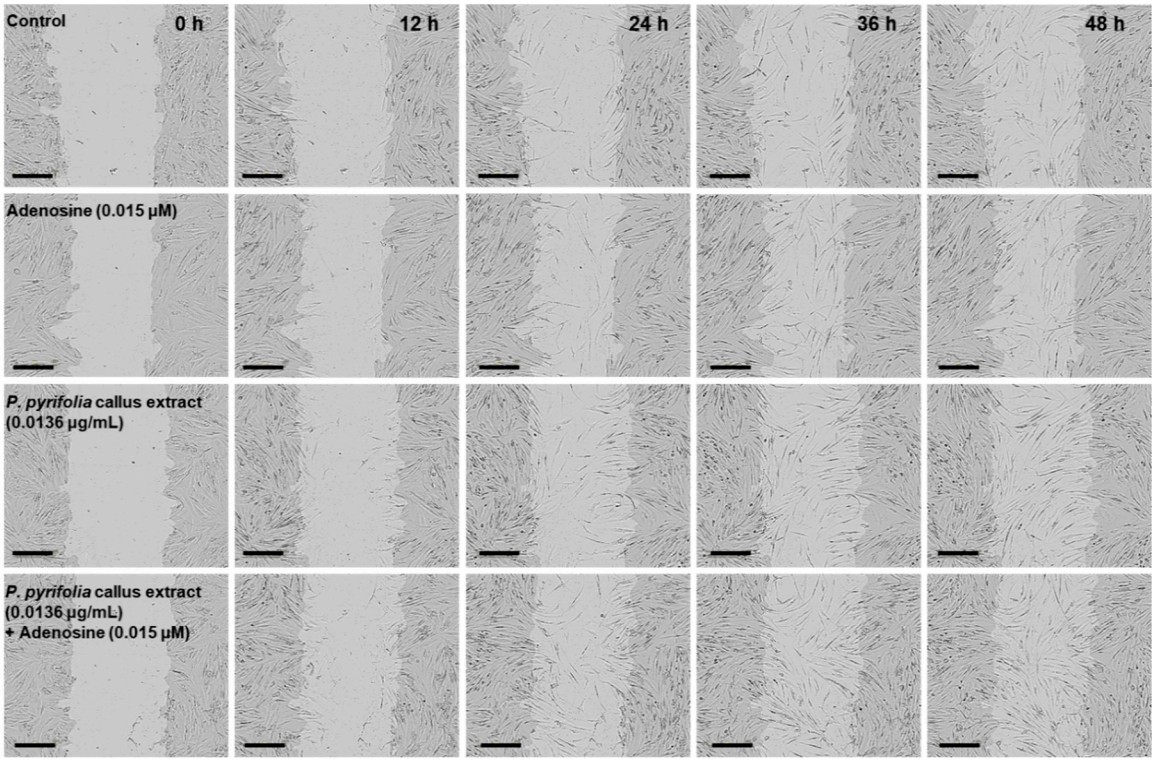

(**c**)

Figure 7. Relative scratch wound recovery of CCD-986sk cells after incubation with adenosine and *P. pyrifolia* callus extract. (**a**) Relative scratch wound recovery of CCD-986sk cells after 36 h. (**b**) Time course of relative scratch wound recovery area of CCD-986sk cells. (**c**) Representative microscopic images of scratch wounds after treatment with serum-free medium (control), adenosine (0.015 μM), or *P. pyrifolia* callus extract (0.0136 μg/mL) alone or in combination with adenosine (0.015 μM). Values are means ± standard deviation (n = 6). * $p < 0.05$, ** $p < 0.01$, *** $p < 0.001$ compared to the untreated control. # $p < 0.05$ compared to adenosine alone (0.015 μM). $$ $p < 0.01$, $$$ $p < 0.001$ compared to *P. pyrifolia* callus extract alone (0.0136 μg/mL). Scale bar in (**c**): 300 μm.

Therefore, the overall results suggest that topical application of callus extract alone and in combination with adenosine has the potential to accelerate the regeneration of damaged skin via stimulation of keratinocyte and fibroblast cell proliferation/migration, activating collagen synthesis and stabilizing the epithelial barrier.

3.4. Characterization and Skin Permeability of P. pyrifolia Callus Extract-Loaded NLs

3.4.1. Characterization of NLs Containing *P. pyrifolia* Callus Extract

To increase the skin permeability of *P. pyrifolia* callus extract, extract-loaded NLs were prepared by emulsification or reverse-phase evaporation followed by microfluidization. All liposomes exhibited ~80% mean entrapment efficacy of callus extract. The mean particle size of the callus extract-loaded liposomes produced by nano-emulsification (PC-NLs) was 96.2 ± 0.6 nm, with a narrow size range distribution (PDI = 0.277 ± 0.009). The zeta potential was −67.2 ± 1.40 mV. The elastic NLs incorporating callus extract (PC-ENLs) produced by thin-film hydration had larger vesicles than PC-NLs, which may have been produced by the incorporation of Tween 80 as an edge activator. The average size and PDI of PC-ENLs were 210 ± 5.8 nm and 0.293 ± 0.021, respectively, and they also had a negative surface charge, with a zeta potential of −43.7 ± 0.890 mV. TEM revealed that all liposomes had nano-sized globular vesicles, and their sizes were similar to the results obtained with a particle size analyzer (Figure 8). TEM images of PC-NLs showed more regular and well-defined

spherical liposomes than PC-ENLs. Most PC-NL vesicles were elliptical in shape with a large interior aqueous phase and a flexible lipid layer.

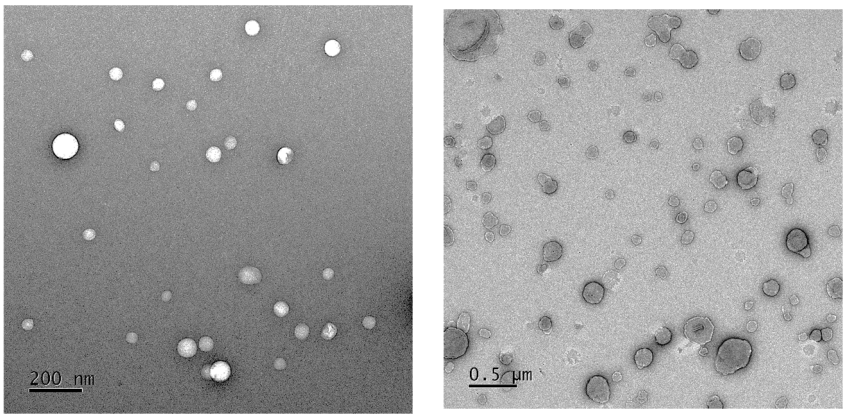

(**a**) (**b**)

Figure 8. Representative transmission electron micrographs of (**a**) *P. pyrifolia* callus extract-loaded nanoliposomes (NLs) produced by nano-emulsification (PC-NLs) and elastic NLs containing callus extract (PC-ENLs). Scale bars in (**a**,**b**): 200 nm and 0.5 μm, respectively.

3.4.2. In Vitro Skin Permeability of NLs Containing *P. pyrifolia* Callus Extract

The artificial skin permeability of *P. pyrifolia* callus extract was significantly increased by encapsulation into NLs (Figure 9). Compared to the skin permeation from *P. pyrifolia* callus extract solution, the permeated concentration values for adenosine in the callus extract from PC-NLs and PC-ENLs were increased by 1.25- and 1.75-fold, respectively, at 24 h (Figure 9a). In addition, the effective permeability of adenosine from PC-ENLs prepared as elastic NLs was significantly greater than those of PC-NLs and callus extract solution, and the maximum skin permeability of adenosine from PC-ENLs was 1.63- and 2.28-fold greater than those of PC-NLs and callus extract alone, respectively ($[0.54 \pm 0.04] \times 10^{-6}$ vs. $[0.33 \pm 0.06] \times 10^{-6}$ vs. $[0.24 \pm 0.07] \times 10^{-6}$ cm/s, respectively).

Elastic NLs are prepared by incorporating a single-chain surfactant as an edge activator, which decreases the transition temperature and destabilizes the lipid bilayers of liposomes, followed by increasing their deformability and elasticity, thereby facilitating skin penetration of liposomes by squeezing them across microlamellar spaces among keratinocytes to penetrate across the skin layer as well as through very tiny pores in the skin [56]. Therefore, enhanced skin permeation of PC-ENLs was also confirmed using an excised human epidermal layer. Incorporation of *P. pyrifolia* callus extract into elastic NLs significantly improved the skin penetration of the callus extract in comparison with callus extract solution (Figure 9b). After a 24-h incubation, the cumulative penetrated concentration of adenosine from the PC-ENL formulation was 24.7-fold higher than that of *P. pyrifolia* callus extract alone. Thus, the skin flux of *P. pyrifolia* callus was increased by 1598% after encapsulation into elastic NEs (3.76 ± 1.71 vs. 0.222 ± 0.326 μg/cm^2/h, respectively).

The enhanced permeability of adenosine from the callus extract could be attributed to the synergistic effects of elastic NLs acting as a carrier. Topically applied elastic NLs have been suggested to interact with the skin, resulting in several sequential events. Initially, water in the dispersion immediately evaporates, which increases the concentration gradient of NLs through the skin, followed by establishing hydration gradients along the skin. Thus, water content in the upper layer increases in comparison to the inner viable epidermis layer, which forms transepidermal hydration gradients. Thereafter, the hydration gradient as well as water affinity and high elasticity of elastic NLs act as driving forces to pull the liposomes toward the inner layer of the skin until they have reached the water-rich viable epidermis. After they have permeated across the SC barrier by diffusion via intercluster and intercorneocyte pathways, the pull mechanism is then changed to push mechanism on the liposomes [56,57]. Furthermore, Subongkot et al. reported that elastic NLs were distinctly present

in the hair follicular region, suggesting that the transfollicular pathway may also play an important role in the release of encapsulated active ingredients, compared to the inter- or trans-cellular route of the nonfollicular region [58]. Thus, *P. pyrifolia* callus extract-loaded elastic NLs may be useful as a potent skin rejuvenating cosmetic preparation exerting an antiaging activity on the skin.

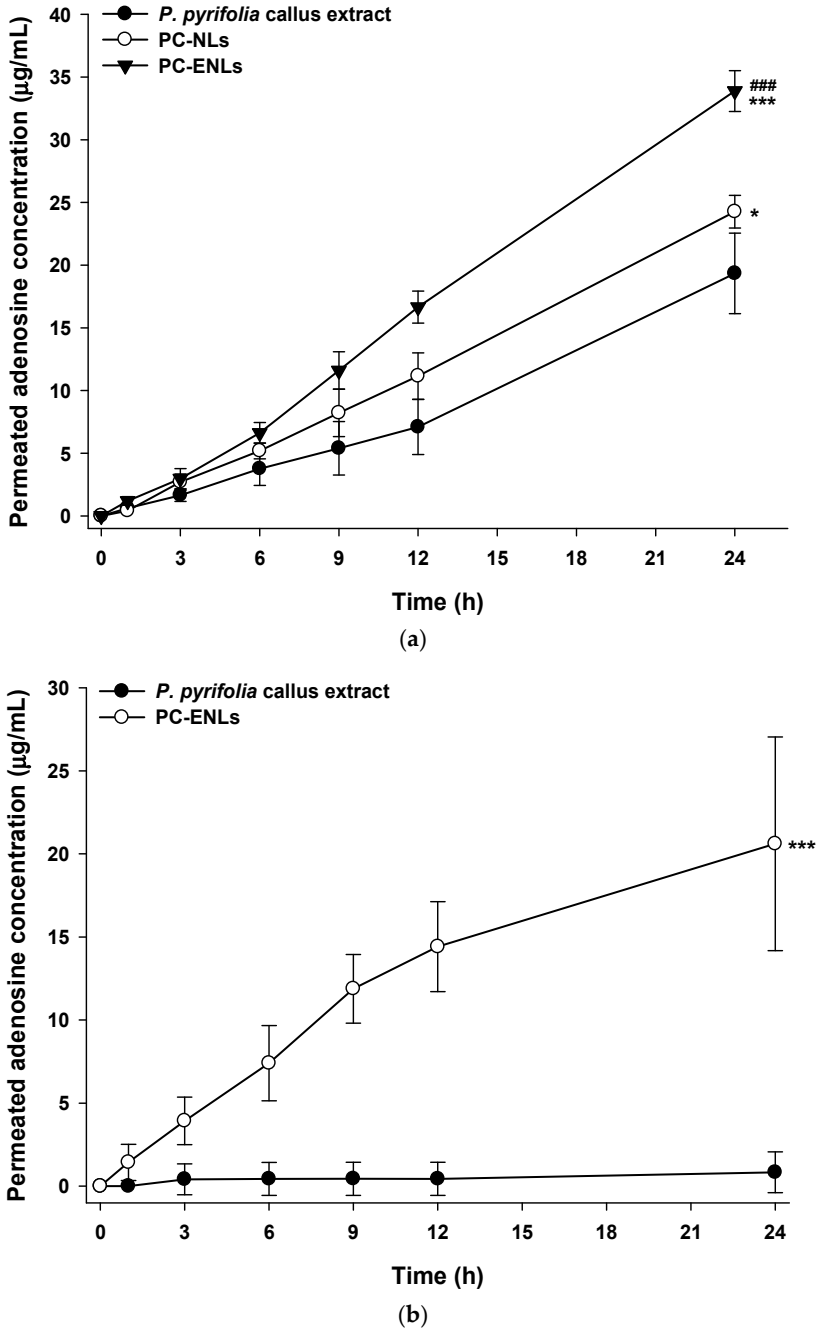

Figure 9. In vitro permeation of *P. pyrifolia* callus extract-loaded nanoliposomes (NLs) across artificial skin (Skin PAMPA) and human epidermal layer. Time course of changes in cumulative permeated concentrations of adenosine from the aqueous solution of callus extract or callus extract-loaded NLs (PC-NLs) or elastic NLs (PC-ENLs) through (**a**) Skin PAMPA and (**b**) human epidermis. Values are means ± standard deviation (n = 6 per group). * $p < 0.05$, *** $p < 0.001$ compared to *P. pyrifolia* callus extract. ### $p < 0.001$ compared to PC-NLs.

4. Conclusions

An aqueous extract was prepared using callus from in vitro-derived leaves of *P. pyrifolia* grown on M&S medium with picloram as a growth regulator. The total phenolic content in the callus extract was 9.25 ± 0.41 gallic acid equivalent/g dried callus extract and the DPPH free radical scavenging activity of the callus extract (300 μg/mL) was equivalent to that of 44 μg/mL ascorbic acid (82.5% ± 3.63%). The major biological components in the callus extract were identified as uridine (**1**), adenosine (**2**), and guanosine (**3**), and the IC_{50} values for inhibition of AGE formation from collagen and elastin were 602 ± 2.72 and 3037 ± 102.5 μg/mL, respectively. The extract significantly promoted keratinocyte and fibroblast proliferation in a dose-dependent manner, and fibroblasts treated with 1.36 μg/mL extract exhibited 1.60- and 1.43-fold increases in the levels of procollagen type I C-peptide compared to controls and cells treated with adenosine (0.015 μM), respectively. The in vitro wound recovery rates of keratinocytes and fibroblasts were also 75% and 38% greater, respectively, than those of serum-free controls at 9 h and 36 h after extract treatment (1.36 μg/mL). Moreover, the combination of extract and adenosine significantly enhanced both cell proliferation/migration and procollagen synthesis. The extract flux across the human epidermis was increased by 1598% after incorporation into elastic NLs. These observations suggest that elastic NLs loaded with *P. pyrifolia* callus extract have potential use as skin rejuvenators and antiaging ingredients in cosmetic formulations.

Author Contributions: Conceptualization, H.J.K. and J.W.P.; methodology, H.J.K.; validation, D.E.P. and D.A.; formal analysis, R.P. and V.K.P.; investigation, H.J.K. and J.W.P.; resources, H.J.K. and J.W.P.; data curation, D.E.P. and D.A.; writing—original draft preparation, D.E.P. and D.A.; writing—review and editing, H.J.K. and J.W.P.; visualization, H.J.K.; supervision, J.W.P.; project administration, H.J.K. and J.W.P.; funding acquisition, J.W.P.

Funding: This research was supported by the Basic Research Program through the National Research Foundation of Korea (NRF), funded by the Ministry of Education (NRF-2017R1D1A1B03032283).

Acknowledgments: We thank BIO-FD&C Co. Ltd. (Hwasun-gun, Jeonnam, Republic of Korea) for their technical support in this research.

Conflicts of Interest: The authors declare no conflict of interest.

References

1. Popoola, O.K.; Marnewick, J.L.; Rautenbach, F.; Ameer, F.; Iwuoha, E.I.; Hussein, A.A. Inhibition of oxidative stress and skin aging-related enzymes by prenylated chalcones and other flavonoids from helichrysum teretifolium. *Molecules* **2015**, *20*, 7143–7155. [CrossRef] [PubMed]
2. Bose, B.; Choudhury, H.; Tandon, P.; Kumaria, S. Studies on secondary metabolite profiling, anti-inflammatory potential, in vitro photoprotective and skin-aging related enzyme inhibitory activities of malaxis acuminata, a threatened orchid of nutraceutical importance. *J. Photochem. Photobiol. B* **2017**, *173*, 686–695. [CrossRef] [PubMed]
3. Pientaweeratch, S.; Panapisal, V.; Tansirikongkol, A. Antioxidant, anti-collagenase and anti-elastase activities of phyllanthus emblica, manilkara zapota and silymarin: An in vitro comparative study for anti-aging applications. *Pharm. Biol.* **2016**, *54*, 1865–1872. [CrossRef] [PubMed]
4. Bravo, K.; Alzate, F.; Osorio, E. Fruits of selected wild and cultivated andean plants as sources of potential compounds with antioxidant and anti-aging activity. *Ind. Crop Prod.* **2016**, *85*, 341–352. [CrossRef]
5. Tu, P.T.; Tawata, S. Anti-oxidant, anti-aging, and anti-melanogenic properties of the essential oils from two varieties of alpinia zerumbet. *Molecules* **2015**, *20*, 16723–16740. [CrossRef] [PubMed]
6. Pinnell, S.R. Cutaneous photodamage, oxidative stress, and topical antioxidant protection. *J. Am. Acad. Dermatol.* **2003**, *48*, 1–19. [CrossRef] [PubMed]
7. Campisi, J. The role of cellular senescence in skin aging. *J. Investig. Dermatol. Symp. Proc.* **1998**, *3*, 1–5.
8. Faragher, R.G.A. Aging & the immune system. *Biochem. Soc. Trans.* **2000**, *28*, 221–226.
9. Rinnerthaler, M.; Bischof, J.; Streubel, M.K.; Trost, A.; Richter, K. Oxidative stress in aging human skin. *Biomolecules* **2015**, *5*, 545–589. [CrossRef]
10. Kasper, M.; Funk, R.H.W. Age-related changes in cells and tissues due to advanced glycation end products (ages). *Arch. Gerontol. Geriatr.* **2001**, *32*, 233–243. [CrossRef]

11. Khazaei, M.R.; Bakhti, M.; Habibi-Rezaei, M. Nicotine reduces the cytotoxic effect of glycated proteins on microglial cells. *Neurochem. Res.* **2010**, *35*, 548–558. [CrossRef] [PubMed]
12. Brownlee, M. Advanced protein glycosylation in diabetes and aging. *Annu. Rev. Med.* **1995**, *46*, 223–234. [CrossRef] [PubMed]
13. Schmidt, A.M.; Stern, D. Atherosclerosis and diabetes: The rage connection. *Curr. Atheroscler. Rep.* **2000**, *2*, 430–436. [CrossRef] [PubMed]
14. Dyer, D.G.; Dunn, J.A.; Thorpe, S.R.; Lyons, T.J.; McCance, D.R.; Baynes, J.W. Accumulation of maillard reaction products in skin collagen in diabetes and aging. *Ann. N. Y. Acad. Sci.* **1992**, *663*, 421–422. [CrossRef] [PubMed]
15. Verzijl, N.; DeGroot, J.; Oldehinkel, E.; Bank, R.A.; Thorpe, S.R.; Baynes, J.W.; Bayliss, M.T.; Bijlsma, J.W.; Lafeber, F.P.; Tekoppele, J.M. Age-related accumulation of maillard reaction products in human articular cartilage collagen. *Biochem. J.* **2000**, *350 Pt 2*, 381–387. [CrossRef]
16. Li, X.; Zhang, J.-Y.; Gao, W.-Y.; Wang, Y.; Wang, H.-Y.; Cao, J.-G.; Huang, L.-Q. Chemical composition and anti-inflammatory and antioxidant activities of eight pear cultivars. *J. Agric. Food Chem.* **2012**, *60*, 8738–8744. [CrossRef] [PubMed]
17. Li, X.; Zhang, J.; Gao, W.; Wang, H. Study on chemical composition, anti-inflammatory and anti-microbial activities of extracts from chinese pear fruit (pyrus bretschneideri rehd.). *Food Chem. Toxicol.* **2012**, *50*, 3673–3679. [CrossRef]
18. Choi, H.J.; Park, J.H.; Han, H.S.; Son, J.H.; Choi, C.; Son, G.M.; Bae, J.H. Effect of polyphenol compound from korean pear (pyrus pyrifolia nakai) on lipid metabolism. *J. Korean Soc. Food Sci. Nutr.* **2004**, *33*, 229–304.
19. Hamauzu, Y.; Forest, F.; Hiramatsu, K.; Sugimoto, M. Effect of pear (pyrus communis l.) procyanidins on gastric lesions induced by hcl/ethanol in rats. *Food Chem.* **2007**, *100*, 255–263. [CrossRef]
20. Huang, L.-J.; Gao, W.-Y.; Li, X.; Zhao, W.-S.; Huang, L.-Q.; Liu, C.-X. Evaluation of the in vivo anti-inflammatory effects of extracts from pyrus bretschneideri rehd. *J. Agric. Food Chem.* **2010**, *58*, 8983–8987. [CrossRef]
21. Lin, L.-Z.; Harnly, J.M. Phenolic compounds and chromatographic profiles of pear skins (pyrus spp.). *J. Agric. Food Chem.* **2008**, *56*, 9094–9101. [CrossRef] [PubMed]
22. Oleszek, W.; Amiot, M.J.; Aubert, S.Y. Identification of some phenolics in pear fruit. *J. Agric. Food Chem.* **1994**, *42*, 1261–1265. [CrossRef]
23. Lee, K.H.; Cho, J.Y.; Lee, H.J.; Ma, Y.K.; Kwon, J.; Park, S.H.; Lee, S.H.; Cho, J.A.; Kim, W.S.; Park, K.H.; et al. Hydroxycinnamoylmalic acids and their methyl esters from pear (pyrus pyrifolia nakai) fruit peel. *J. Agric. Food Chem.* **2011**, *59*, 10124–10128. [CrossRef] [PubMed]
24. Lee, K.H.; Cho, J.-Y.; Lee, H.J.; Park, K.Y.; Ma, Y.-K.; Lee, S.-H.; Cho, J.A.; Kim, W.-S.; Park, K.-H.; Moon, J.-H. Isolation and identification of phenolic compounds from an asian pear (pyrus pyrifolia nakai) fruit peel. *Food Sci. Biotechnol.* **2011**, *20*, 1539–1545. [CrossRef]
25. Ma, J.-N.; Wang, S.-L.; Zhang, K.; Wu, Z.-G.; Hattori, M.; Chen, G.-L.; Ma, C.-M. Chemical components and antioxidant activity of the peels of commercial apple-shaped pear (fruit of pyrus pyrifolia cv. Pingguoli). *J. Food Sci.* **2012**, *77*, C1097–C1102. [CrossRef]
26. Li, X.; Wang, T.; Zhou, B.; Gao, W.; Cao, J.; Huang, L. Chemical composition and antioxidant and anti-inflammatory potential of peels and flesh from 10 different pear varieties (pyrus spp.). *Food Chem.* **2014**, *152*, 531–538. [CrossRef] [PubMed]
27. Kim, H.Y.; Kim, K. Protein glycation inhibitory and antioxidative activities of some plant extracts in vitro. *J. Agric. Food Chem.* **2003**, *51*, 1586–1591. [CrossRef] [PubMed]
28. Barbulova, A.; Apone, F.; Colucci, G. Plant cell cultures as source of cosmetic active ingredients. *Cosmetics* **2014**, *1*, 94–104. [CrossRef]
29. Fazal, H.; Abbasi, B.H.; Ahmad, N. Optimization of adventitious root culture for production of biomass and secondary metabolites in prunella vulgaris L. *Appl. Biochem. Biotechnol.* **2014**, *174*, 2086–2095. [CrossRef]
30. Ahmad, N.; Rab, A.; Ahmad, N. Light-induced biochemical variations in secondary metabolite production and antioxidant activity in callus cultures of stevia rebaudiana (bert). *J. Photochem. Photobiol. B* **2016**, *154*, 51–56. [CrossRef]
31. Grąbkowska, R.; Matkowski, A.; Grzegorczyk-Karolak, I.; Wysokińska, H. Callus cultures of harpagophytum procumbens (burch.) dc. Ex meisn.; production of secondary metabolites and antioxidant activity. *S. Afr. J. Bot.* **2016**, *103*, 41–48. [CrossRef]

32. Debnath, M.; Malik, C.P.; Bisen, P.S. Micropropagation: A tool for the production of high quality plant-based medicines. *Curr. Pharm. Biotechnol.* **2006**, *7*, 33–49. [CrossRef] [PubMed]
33. Espinosa-Leal, C.A.; Puente-Garza, C.A.; García-Lara, S. In vitro plant tissue culture: Means for production of biological active compounds. *Planta* **2018**, *248*, 1–18. [CrossRef] [PubMed]
34. Fischer, R.; Vasilev, N.; Twyman, R.M.; Schillberg, S. High-value products from plants: The challenges of process optimization. *Curr. Opin. Biotechnol.* **2015**, *32*, 156–162. [CrossRef] [PubMed]
35. Vinardell, M.P.; Mitjans, M. Nanocarriers for delivery of antioxidants on the skin. *Cosmetics* **2015**, *2*, 342–354. [CrossRef]
36. Singleton, V.L.; Rossi, J.A. Colorimetry of total phenolics with phosphomolybdic-phosphotungstic acid reagents. *Am. J. Enol. Vitic.* **1965**, *16*, 144–158.
37. Zhishen, J.; Mengcheng, T.; Jianming, W. The determination of flavonoid contents in mulberry and their scavenging effects on superoxide radicals. *Food Chem.* **1999**, *64*, 555–559. [CrossRef]
38. Adhikari, D.; Panthi, V.K.; Pangeni, R.; Kim, H.J.; Park, J.W. Preparation, characterization, and biological activities of topical anti-aging ingredients in a citrus junos callus extract. *Molecules* **2017**, *22*, 2198. [CrossRef]
39. Brand-Williams, W.; Cuvelier, M.E.; Berset, C. Use of a free radical method to evaluate antioxidant activity. *LWT-Food Sci. Technol.* **1995**, *28*, 25–30. [CrossRef]
40. Re, R.; Pellegrini, N.; Proteggente, A.; Pannala, A.; Yang, M.; Rice-Evans, C. Antioxidant activity applying an improved abts radical cation decolorization assay. *Free Radic. Biol. Med.* **1999**, *26*, 1231–1237. [CrossRef]
41. Pulido, R.; Bravo, L.; Saura-Calixto, F. Antioxidant activity of dietary polyphenols as determined by a modified ferric reducing/antioxidant power assay. *J. Agric. Food Chem.* **2000**, *48*, 3396–3402. [CrossRef] [PubMed]
42. Oh, J.Y.; In, Y.S.; Kim, M.K.; Ko, J.H.; Lee, H.J.; Shin, K.C.; Lee, S.M.; Wee, W.R.; Lee, J.H.; Park, M. Protective effect of uridine on cornea in a rabbit dry eye model. *Invest. Ophthalmol. Vis. Sci.* **2007**, *48*, 1102–1109. [CrossRef] [PubMed]
43. Abella, M.L. Evaluation of anti-wrinkle efficacy of adenosine-containing products using the foits technique. *Int. J. Cosmet. Sci.* **2006**, *28*, 447–451. [CrossRef] [PubMed]
44. Souza, D.G.; Bellaver, B.; Bobermin, L.D.; Souza, D.O.; Quincozes-Santos, A. Anti-aging effects of guanosine in glial cells. *Purinergic Signal.* **2016**, *12*, 697–706. [CrossRef] [PubMed]
45. Dzialo, M.; Mierziak, J.; Korzun, U.; Preisner, M.; Szopa, J.; Kulma, A. The potential of plant phenolics in prevention and therapy of skin disorders. *Int. J. Mol. Sci.* **2016**, *17*, 160. [CrossRef] [PubMed]
46. Hariprasath, L.; Jegadeesh, R.; Arjun, P.; Raaman, N. In vitro propagation of senecio candicans dc and comparative antioxidant properties of aqueous extracts of the in vivo plant and in vitro-derived callus. *S. Afr. J. Bot.* **2015**, *98*, 134–141. [CrossRef]
47. Velioglu, Y.S.; Mazza, G.; Gao, L.; Oomah, B.D. Antioxidant activity and total phenolics in selected fruits, vegetables, and grain products. *J. Agric. Food Chem.* **1998**, *46*, 4113–4117. [CrossRef]
48. López-Laredo, A.R.; Gómez-Aguirre, Y.A.; Medina-Pérez, V.; Salcedo-Morales, G.; Sepúlveda-Jiménez, G.; Trejo-Tapia, G. Variation in antioxidant properties and phenolics concentration in different organs of wild growing and greenhouse cultivated castilleja tenuiflora benth. *Acta Physiol. Plant.* **2012**, *34*, 2435–2442. [CrossRef]
49. Lee, S.-H.; Cho, J.-Y.; Jeong, H.Y.; Jeong, D.E.; Kim, D.; Cho, S.-Y.; Kim, W.-S.; Moon, J.-H. Comparison of bioactive compound contents and in vitro and ex vivo antioxidative activities between peel and flesh of pear (pyrus pyrifolia nakai). *Food Sci. Biotechnol.* **2015**, *24*, 207–216. [CrossRef]
50. Sadowska-Bartosz, I.; Bartosz, G. Prevention of protein glycation by natural compounds. *Molecules* **2015**, *20*, 3309–3334. [CrossRef]
51. Valls, M.D.; Cronstein, B.N.; Montesinos, M.C. Adenosine receptor agonists for promotion of dermal wound healing. *Biochem. Pharmacol.* **2009**, *77*, 1117–1124. [CrossRef] [PubMed]
52. Chan, E.S.; Fernandez, P.; Merchant, A.A.; Montesinos, M.C.; Trzaska, S.; Desai, A.; Tung, C.F.; Khoa, D.N.; Pillinger, M.H.; Reiss, A.B.; et al. Adenosine a2a receptors in diffuse dermal fibrosis: Pathogenic role in human dermal fibroblasts and in a murine model of scleroderma. *Arthritis Rheum.* **2006**, *54*, 2632–2642. [CrossRef] [PubMed]
53. Hartinger, J.; Vesely, P.; Netikova, I.; Matouskova, E.; Petruzelka, L. The protective effect of pyrimidine nucleosides on human hacat keratinocytes treated with 5-fu. *Anticancer Res.* **2015**, *35*, 1303–1310. [PubMed]

54. Jin, H.; Seo, J.; Eun, S.Y.; Joo, Y.N.; Park, S.W.; Lee, J.H.; Chang, K.C.; Kim, H.J. P2y2 r activation by nucleotides promotes skin wound-healing process. *Exp. Dermatol.* **2014**, *23*, 480–485. [CrossRef] [PubMed]
55. Clark, A.N.; Youkey, R.; Liu, X.; Jia, L.; Blatt, R.; Day, Y.J.; Sullivan, G.W.; Linden, J.; Tucker, A.L. A1 adenosine receptor activation promotes angiogenesis and release of vegf from monocytes. *Circ. Res.* **2007**, *101*, 1130–1138. [CrossRef] [PubMed]
56. Hussain, A.; Singh, S.; Sharma, D.; Webster, T.J.; Shafaat, K.; Faruk, A. Elastic liposomes as novel carriers: Recent advances in drug delivery. *Int. J. Nanomed.* **2017**, *12*, 5087–5108. [CrossRef] [PubMed]
57. Chen, J.; Lu, W.-L.; Gu, W.; Lu, S.-S.; Chen, Z.-P.; Cai, B.-C. Skin permeation behavior of elastic liposomes: Role of formulation ingredients. *Expert Opin. Drug Deliv.* **2013**, *10*, 845–856. [CrossRef]
58. Subongkot, T.; Pamornpathomkul, B.; Rojanarata, T.; Opanasopit, P.; Ngawhirunpat, T. Investigation of the mechanism of enhanced skin penetration by ultradeformable liposomes. *Int. J. Nanomed.* **2014**, *9*, 3539–3550. [CrossRef]